universität wien

# MASTERARBEIT

Titel der Masterarbeit

„Neuroimaging of Social Anxiety Disorder“

Verfasserin

Lora Guintcheva Minkova, M.A.

angestrebter akademischer Grad

Master of Science (M.Sc.)

Wien, 2013

Studienkennzahl lt. Studienblatt: A 066 013

| | |
|---|---|
| Studienrichtung lt. Studienblatt: | Middle European Interdisciplinary Master Programme in Cognitive Science (MEi:CogSci) |
| Betreuerin / Betreuer: | Ronald Sladky, PhD<br>MR Centre of Excellence, Medical University of Vienna |

# Table of Contents

## Abstract

Social anxiety disorder (SAD), or social phobia, is a serious psychiatric health problem which can have a devastating impact on a person's life and well-being. The current thesis seeks to incorporate a broader multidisciplinary approach in the study of SAD by integrating different scientific traditions from various disciplines into one framework. The main focus is on the neuronal underpinnings of SAD during emotional perception and its impact on cognition and vice versa. Further evidence for currently studied neurobiological models of affective processing in SAD patients will undoubtedly broaden our understanding of the disorder and facilitate further advancements in therapeutic approaches and interventions. While the outcomes of our experimental study did not contradict current neuroimaging findings on SAD, we did not observe the expected results, such as a clear identification of alternations within the limbic-cortical network in patients relative to healthy control participants. Suggestions for improvements and further work are discussed at the end of the thesis.



## Kurzfassung

Soziale Angststörung (soziale Phobie) ist eine psychiatrische Erkrankung, die schädliche Dauerauswirkungen auf das Leben und Wohlbefinden des erkrankten Menschen hat. Die folgende Masterarbeit zielt auf einen breiteren multidisziplinären Ansatz ab, der verschiedene wissenschaftliche Traditionen für die Untersuchung von sozialer Phobie vereint. Der Schwerpunkt liegt dabei auf der neuronalen Grundlage der sozialen Phobie sowie auf dem Zusammenspiel zwischen Emotion und Kognition. Ein weiterer Beweis für die derzeit untersuchten neurobiologischen Modelle über die affektive Verarbeitung bei Phobiepatienten wird zweifellos das Verständnis für die Erkrankung erleichtern und gleichfalls zur Weiterentwicklung im therapeutischen Bereich führen. Trotz, dass die Ergebnisse unserer experimentellen Studie den aktuellen bildgebenden Befunden nicht widersprachen, konnten wir keine eindeutigen Unterschiede des affektiven neuronalen Netzwerks von gesunden Probanden zu Phobiepatienten identifizieren. Verbesserungsvorschläge und weitere wissenschaftlichen Arbeiten werden am Ende der Masterarbeit diskutiert.

## Acknowledgements

First and foremost, I would like to express my deepest gratitude to my supervisor Dr. Ronald Sladky for all his support and patience during the whole process of the master thesis. Without his guidance and constructive criticisms this work would have been impossible.

I take this opportunity to convey my sincere thanks to Prof. Dr. Markus Peschl, Brigitte Roemmer-Nossek and Elisabeth Zimmermann for the interesting and enlightening study programme and all their indispensable support in administrative and organisational matters. I would also like to thank all my teachers and colleagues for their stimulating input and for helping me broaden my view and knowledge.

I owe a special debt of gratitude to my family and friends for their support and encouragement in difficult moments.

# List of Figures and Tables

# I. Introduction

Emotions are an indispensable part of our everyday lives and have been a topic of extensive research for ages. The study of emotions has been influenced by a number of different scientific traditions, each contributing to the understanding of emotions and transforming their study into a multidisciplinary endeavour.

## *1.1. The Study of Emotions: A Brief Historical Overview*

Within the philosophical tradition, two philosophers of great importance for the study of emotions should be mentioned: Plato and Aristotle. Although they both recognised the existence of emotion and cognition, their views differed significantly with reference to the nature of emotions and their impact on cognition. Plato's tripartite theory of the soul, composed of reason, spirit and appetite, suggested that reason (aided by spirit) is superior to appetite, thus treating emotions as detrimental to cognition. In contrast, Aristotle suggested that emotions and rationality need not be opposed to each other and emotions serve a certain psychological purpose and therefore involve cognition. While the Aristotelian functionalist theory of emotions can be regarded as the predecessor of today's cognitive theories, it was Plato's theory of mind that influenced further theoretical work that dominated the scene until the middle of the twentieth century.

An important turn in the study of emotions was caused by the evolutionary tradition, associated with the work of Charles Darwin[1]. While philosophers like Descartes believed that only humans have emotions[2], Darwin argued that basic emotions are universal and are linked to natural selection in that they increase the chances of survival, without the necessity for higher order cognition as proposed to

[1] *The Expression of Emotions in Man and Animals* (1872)
[2] Descartes suggested that dogs are merely biological machines, unable to feel.

Plato's idea. Darwin's evolutionary reading of emotions gave rise to a lot of research on the universality of facial expressions and of emotions among different species and resulted in later disciplines such as evolutionary psychiatry. Within the realm of psychiatry, an important role played the work of Sigmund Freud and his interpretation of emotions as complex, generally unconscious to the individual, states involving early experiences, personal traits and conflicts, and defence mechanisms. His views on emotions raised, for instance, the question whether emotions are unconscious or if awareness is a necessary part in the emotional process.

Another influential tradition, the psycho-physiological one, which completely excluded the role of cognition, has its roots in the work of the American psychologist-philosopher William James (1884). According to the James-Lange theory of emotions (Cannon, 1927)[3], the visceral changes of the body (e.g. increased heart rate) and the context of a certain situation (e.g. an approaching bear) give rise to the corresponding emotion (e.g. fear). In other words, one feels afraid because the heart beats faster. One of the main arguments against this theory was that it could not explain how emotions arising from the same or similar bodily changes can be distinguished from one another. Although James' ideas have been refuted, they were important because they raised awareness about the psycho-physiological processes related to emotions. As far as cognition is concerned, however, it was still not considered an important part of the emotional process. Similarly, the behaviourist paradigm, which dominated the scientific scene during the first part of the twentieth century, further limited the research on unobservable phenomena such as mental states and emotions and put its focus primarily on behaviour (Power & Dalgleish, 2008).

[3] James and Lange developed their theories independently but, owing to their shared fundamental notions of emotions, their theories were later unified and referred to as James-Lange theory.

The James-Lange theory has also had an influence on the work of another scientist, the physiologist Walter Cannon, who can be seen as the founder of the neurological tradition in the study of emotions. He showed experimentally on dogs and cats that the autonomic nervous system (ANS) is not a prerequisite for the presence of emotions and the animals in his experiments could still show typical emotional reactions even in the absence of entire divisions of the ANS. Instead, he suggested that the thalamus is the source of emotional feelings. Although Cannon's view of emotions had its limitations, it was crucial for the research on the neuroanatomical circuits of and interaction between emotion and cognition (Power & Dalgleish, 2008).

The cognition-emotion debate took another turn in the second part of the twentieth century, following the cognitive revolution of the 1960s (Plutchik, 2003). Although the cognitive tradition recognised the role of cognition for the processing of emotions, there was, and still is, a lack of consensus about the relation between the two. For instance, the importance of an individual's interpretation of a situation, also often referred to as an appraisal, has been emphasised by a number of scientists. An example is the research of Schachter and Singer (1962), who used epinephrine injections to elicit physiological manifestations. According to their two-factor theory, emotion requires both cognitive factors and physiological arousal, i.e. people look for emotionally relevant cues within their environment in order to explain their physiological arousal.

Similarly, the American psychologist Magda Arnold, who was the first to develop the appraisal theory of emotions in the 1960s, suggested that appraisal is not only a requirement, but also precedes emotions (see Shields & Kappas, 2006 for a more detailed discussion). Another illustration of the question whether emotions

can occur without or before appraisal is evident from the Zajonc-Lazarus debate. Zajonc was a supporter of the affective primacy hypothesis, suggesting that emotions occur before cognition and cognitive processes can influence emotions but at a later stage (Zajonc, 1980), while Lazarus insisted that cognitive appraisal is a prerequisite for emotions (Lazarus, 1981).

The Zajonc-Lazarus debate was settled by the experimental work of LeDoux (1984) on fear conditioning, suggesting two pathways – fast processing of stimuli by the amygdala to support the survival of the individual and slower processing involving the neocortex, responsible for 'higher' cognitive processes. Damasio, on the other hand, proposed another dichotomy: primary emotions, which are biologically primitive and are unconsciously induced without cognition, versus secondary emotions, which are associated with cognition (Damasio, 1994). In other words, primary emotions are unconscious and are associated with the amygdala, while secondary emotions require consciousness and involve the prefrontal cortex (Adolphs & Damasio, 2000).

It seems obvious that attention in a necessary requirement for consciousness and therefore it should also play an essential role for emotional processing. Posner and Peterson (1990) distinguish between selective attention, i.e. consciously attending to certain stimuli, and vigilance, e.g. the state of alertness to potential danger, which can be regarded as unconscious. Furthermore, attention can be divided into exogenous or stimulus-driven, involving bottom-up processing, and endogenous or executive attention, which involves top-down processing. This is also consistent with the two pathways of processing proposed by LeDoux (1984).

Although there is obviously a link between attention and emotional perception, there has been a lot of disagreement about how the former modulates the latter and vice versa. On the one hand, some studies suggest that emotional perception is

automatic and occurs irrespective of attentional load. For example, it was shown in a visual search MEG experiment that fearful faces attract attention in an automatic bottom-up fashion, independent of other task-relevant attentional operations (Fenker et al., 2010). To confirm the prioritisation of emotional processing, no processing resources should be available, which will confirm that attention is not necessary for emotional perception to occur. On the other hand, there is also evidence that emotional perception depends on attention and the availability of processing resources and is affected by attentional load (Mitchell et al., 2007; Schupp, Junghöfer, Weike, & Hamm, 2003; Silvert et al., 2007). For instance, an fMRI study investigating how demanding peripheral tasks influence the processing of centrally presented emotional faces showed that the valence effect (e.g. fearful > neutral) was only observable during low task demand conditions, but not during medium or high demand ones. Furthermore, signal decreases in amygdala were observed during demanding non-emotional tasks, suggesting the attenuating effect of attentional and cognitive load on affective processing (Pessoa, Padmala, & Morland, 2005).

## *1.2. Aim of Thesis and Outline*

The complex and multi-facetted nature of emotions and the above-discussed scientific traditions, as well as the recent technological advancements, have transformed the study of emotions into a challenging but also manifold and exciting endeavour. Within the scope of the current master thesis, an affective psychiatric disorder known as social phobia or social anxiety disorder (SAD) will be investigated using a multidisciplinary approach.

The master thesis will be divided into three main parts and will engage different views from the fields of cognitive science, psychology, psychiatry,

neurobiology, and medical physics, among others. In the first part, an overview of the phenomenon of social anxiety disorder will be discussed, including definition of the disorder, symptoms, diagnosis and prevalence, as well as treatment possibilities. Furthermore, the neurobiology of anxiety and the neurobiologically plausible models relying on lesion studies, both involving human patients and animal studies, will be described. In addition, cognitive models of anxiety, supporting findings and outcomes from psychiatric therapies, will be mentioned.

Although lesion studies deliver valuable information about the functioning of the brain, they also face various limitations. For instance, lesions resulting from brain pathologies are rarely limited to only one particular brain area and damage often leads to impairment of different neural circuits simultaneously. Furthermore, the neural circuits have a distributed character and possess plasticity properties, which offer the opportunity for the brain to adjust and use other regions in order to recover from damage. Therefore, the information acquired from lesion studies, which is undoubtedly valuable, should be further used to create formal models that can be tested on both patients and healthy individuals using, for instance, neuroimaging techniques such as functional magnetic resonance imaging (fMRI), a well-established and widely accepted method in science mainly due to its non-invasiveness and relatively good spatial resolution.

The second part of the thesis provides an introduction into the methodology of fMRI, which is the neuroimaging method used for the study described in the third part of the thesis. Specifically, the methodological part includes: a short overview of the physical principles of the magnetic resonance imaging (MRI), the nature of the blood oxygenation dependent functional MRI (BOLD fMRI), fMRI study designs, data pre-processing, and data analysis. While a comprehensive overview of the fMRI

methodology is out of the scope of this thesis, the methodological part should serve as a concise introduction to people who are not acquainted with fMRI and should allow for a better understanding of the approach used for the empirical study at the end of the thesis.

The third and last part will focus on an event-related fMRI experiment conducted with patients suffering from social anxiety disorder and healthy control participants. The study aims at investigating the relationship and interplay between cognition and emotion by exploring the effects of emotional distractors on cognitive tasks. For this purpose, a modified emotional Stroop test will be used, which is adapted from a similar study conducted by Blair and colleagues (Blair et al., 2007). Specifically, pictures of harsh and neutral faces will serve as distractors in a cognitive task involving a numerical discrimination Stroop task and two hypotheses regarding the bottom-up and top-down emotional processing will be tested. First, it will be investigated whether the amygdala is more hyperactive in SAD patients relative to healthy participants during perception of harsh faces, irrespective of the attentional load. The attentional load will be varied using three different conditions: congruent and incongruent tasks and fixation (no task, aka. fueling condition). The second hypothesis suggests that the anxiety-induced activation of the limbic system, and particularly the hyper-activation of the amygdala, is down-regulated by prefrontal brain areas. While the down-regulation mechanism is ought to function properly in healthy participants, it is supposedly impaired in SAD patients.

# II. Theoretical Approach

## *2.1. Social Anxiety Disorder*

### 2.1.1. Definition and symptoms

Social Anxiety Disorder (SAD), also known as social phobia, is a psychiatric condition officially recognised in the 1980s by the American Psychiatric Association (APA, 1980). SAD is characterised by extreme emotional distress in social situations, often caused by low self-esteem and the fear of being judged and criticised by others. People with social anxiety disorder avoid social situations such as meeting new people, being in the centre of attention, being watched while doing something, eating or drinking in public, public speaking, making small talk, talking to important people or authority figures, making phone calls, and attending parties or other social gatherings.

However, it can be argued that some of the above-mentioned social situations (e.g. public speaking) are often experienced as extremely stressful by a large number of people, which does not imply that they all suffer from SAD. In order for such a situation to be classified as phobic, it should have lasting severe and distressful effects for the individual. Moreover, not necessarily all of the above situations should be regarded as phobic by the person. In fact, individuals can suffer from specific/discrete SAD (e.g. phobia in certain situations only, like in public speaking) or from generalised/defused SAD, in which case anxiety is experienced in most social situations.

SAD is usually accompanied with a number of bodily symptoms including blushing, sweating, heart racing, trembling, persistent nervousness, dizziness, nausea, and even panic attacks. Although SAD patients often recognise that their

fear is unreasonable and excessive, they find it difficult to cope with it and tend to avoid feared situations, which can have a great impact on their social activities and relationships, as well as on their normal personal routine, health, and occupational or academic choice. This inability to cope with social anxiety may suggest the presence of bottom-up emotional processes independent of cognition (i.e. feeling anxious although realising that the fear is unreasonable).

As far as the definition and symptoms linked to SAD are concerned, it is interesting to mention that Kashdan and McKnight (2010) have recently proposed the existence of a subtype of people suffering from social phobia who deviate from the prototypical SAD patient. In addition to the stereotypically shy, submissive, inhibited, and risk-avoiding SAD patient, there seems to be a subgroup of people who are characterised as aggressive, impulsive and risk seekers. Since these people differ so strongly from the typical individuals with SAD and are more unlikely to seek for help, their numbers are difficult to estimate. In fact, the authors argue that such a subgroup put the present psychiatric practice and treatments in question. Indeed, further research on this issue is needed to confirm the necessity for modifying the generally accepted diagnostic and treatment practice.

### 2.1.2. Diagnosis and prevalence

Nowadays, SAD is considered the third largest psychiatric health problem worldwide, after depression and alcohol dependence (APA, 2000). SAD is diagnosed according to either DSM-IV 300.23 (Diagnostic and Statistical Manual of Mental Disorders published by the APA, last revision: 2000) or ICD-10 F 40.1 (International Classification of Diseases by the World Health Organisation, 1990). Despite the great similarity between the two tools, the diagnostic criteria slightly differ, with ICD-10 considered having the more stringent criteria. For instance, ICD-10 does not include

public speaking as a phobic situation because fear of scrutiny needs to be related to small groups of people. Furthermore, the socio-economic burden on individuals with regard to occupational impairment resulting from SAD is central to DSM-IV, but not to ICD-10.

A recent epidemiological data for Europe[4] found a 12-month prevalence rate of 2.3 % (Wittchen et al., 2011) and lifetime prevalence rate of 3.9 to 13.7 %. (Fehm, Pelissolo, Furmark, & Wittchen, 2005). Similar results were also published for the United States: a 12-month prevalence rate of 7.1 % and lifetime prevalence rate of 12.1 % (Ruscio et al., 2008). The typical age onset is considered to be adolescence (age of 14+), although it is also possible for SAD to occur later, following some social trauma or extreme social pressure. With regard to gender differences, the risk for women to develop SAD is higher than for men, with a female-to-male ratio of 3:2 (Fehm et al., 2005). However, this trend has not been confirmed by all studies and some clinical samples have shown no gender differences or even slightly higher scores for men (see Fehm et al., 2005). As far as heritability is concerned, there are no conclusive results. While several studies seem to provide evidence for the familial transmission of SAD (Kendler, Karkowski, & Prescott, 1999; Mancini, van Ameringen, Szatmari, Fugere, & Boyle, 1996; Stein et al., 1998), these findings may also be influenced by environmental factors, which are difficult to exclude. In order to confirm the heritability of SAD, a wider scope of twin studies would be recommended.

A common characteristic of SAD is its high degree of commorbidity with other psychiatric conditions (Wittchen & Fehm, 2003). In particular, depression and other anxiety disorders are consistently associated with SAD. Furthermore, SAD often precedes major depression and substance abuse, although the relationship is not

[4] Data were collected from the EU member countries, as well as Switzerland, Iceland and Norway.

necessarily temporal, but can also be causal. The complexity of SAD suggests that impairment cannot always be clearly attributed to SAD, which also affects treatment approaches and evaluation of risk factors and degree of disability. Generally, although the clinical diagnosis of SAD does not pose significant difficulties, the causes for SAD are not yet entirely understood.

### 2.1.3. Intervention and treatment

A major problem of treating SAD results from the nature of the disorder itself. Specifically, a large number of affected individuals avoid seeking medical help partly because they feel embarrassed and are afraid of what others might think about them. Unfortunately, this leads to a vicious circle characterised by worsening of the disorder and even rarer help-seeking behaviour. Consequently, the more severe the disorder is, the less effective the treatment proves to be. Public awareness may possibly have a positive impact on the treatment-seeking behaviour of SAD patients.

The typical treatment options for SAD patients are psychotherapy and medication, or a combination of both. One of the most influential psychotherapeutic approaches is the so-called cognitive behaviour therapy. It is based on the assumption that various cognitive biases determine the vulnerability of individuals to depressive and anxiety disorders (Beck & Clark, 1997; Williams, 1997). These cognitive biases can be attentional (selective attention to threat-related stimuli relative to neutral ones), interpretive (interpretation of ambiguous stimuli as threat-related), explicit memory (the tendency to consciously recollect negative rather than positive or neutral information), and implicit memory (better performance on memory tests involving unconscious recollection of negative stimuli rather than neutral and positive ones).

Cognitive behaviour therapy (CBT) basically aims at changing the patient's negative thoughts and submissive behaviours and has proven highly effective in treating SAD (Acarturk, Cuijpers, van Straten, & Graaf, 2009; Hofmann & Smits, 2008). It can be conducted in a group or individually, although, due to the fear of judgement typical for SAD, one-to-one CBT proves to be more effective. CBT may include different techniques such as exposure (e.g. to phone or eating fears) or cognitive restructuring. Within the framework of the exposure technique, the patient imagines an anxiety-inducing situation, which is usually avoided in everyday life, and practises how to overcome it in order to learn to apply the same strategies in real-life situations. Cognitive restructuring, on the other hand, focuses on the identification of negative thoughts, low self-esteem and negative attribution biases (i.e. attributing success to luck, while failure to personal traits), which are then evaluated and alternative thoughts are identified to restructure the original ones. In addition to CBT, social skills training and relaxation exercises may also be useful to individuals suffering from SAD. CBTs are based on cognitive models of anxiety, which will be discussed in more detail later.

With regard to medication options, serotonin reuptake inhibitors (SSRIs), a type of antidepressants, are among the most frequently prescribed medications. Other antidepressants used for treating SAD are the serotonin-norepinephrine reuptake inhibitors (SNRIs), which act on both serotonergic and adrenergic neurotransmitter systems. In addition, beta blockers, which help diminish the effects of epinephrine, may be used infrequently at a particular anxiety-inducing situation, as they reduce physiological symptoms such as increased heart rate and blood pressure. Finally, oxidase inhibitors (MAOs), which increase synaptic levels of dopamine, serotonin and norepinephrine, and benzodiazepines, which enhance the

activity of the inhibitory neurotransmitter GABA, have also been prescribed to SAD patients in the past, although their use is nowadays often avoided due to their side-effects (e.g. benzodiazepines have a sedative and habit-forming effect, while the intake of MAOs is incompatible with certain foods).

Medical treatment possibilities are based on extensive research on the neurobiological mechanisms of SAD, which will be discussed in the following section.

### 2.1.4. Neurobiology of SAD

On a molecular level, several neurotransmitter systems, including GABA, glutamate, serotonin, dopamine, epinephrine and norepinephrine, seem to be involved in SAD, but also in other comorbid disorders such as major depressive disorder and panic disorder (Hoffman & Mathew, 2008; Vaswani, Linda, & Ramesh, 2003). Hyperactivity of the hypothalamic-pituitary-adrenal-axis (HPA-axis), which is also linked to the modulation of the serotonergic and dopaminergic neurotransmitter systems, is also believed to play a role in mood and anxiety disorders (Mantella et al., 2008), although other neuroendocrine studies failed to confirm any HPA-axis alteration specific to SAD (Martel et al., 1999; Uhde, Tancer, Gelernter, & Vittone, 1994).

To date, the serotonergic and dopaminergic neurotransmitter systems, which are known to modulate the activity of excitatory (e.g. glutamate) and inhibitory (GABA) neurotransmitters, have received a particular attention in the SAD research. The efficacy of SSRIs for the treatment of SAD has suggested that the serotonin has an important role in SAD and findings from both animal studies and studies with SAD patients further support this assumption. For instance, a comprehensive study by Lanzenberger and colleagues (2007) has demonstrated that SAD patients have lower serotonin-1A receptor binding in amygdala, anterior cingulate cortex (ACC), insula, and dorsal raphe nuclei.

In addition to serotonin, SSRIs seem to affect the dopaminergic neurotransmitter system. For instance, studies have shown that administration of SSRIs leads to increased dopamine transporter (DAT) binding (Warwick et al., 2012; Willner, Hale, & Argyropoulos, 2005). However, the findings are inconsistent and while some studies have found decreased striatal DAT and D2 receptor availability in SAD patients (Schneier et al., 2000; Tiihonen et al., 1997), others suggest an increased binding potential for DAT in the striatum (van der Wee et al., 2008). Although there is clearly serotonergic and dopaminergic dysfunction in patients with SAD, the exact mechanisms of these neurotransmitter systems are still not clear and are a topic of current research.

Serotonergic and dopaminergic neurons innervate various brain regions, including the prefrontal cortex, striatum, thalamus, and amygdala (Li, Chokka, & Tibbo, 2001). Studies focusing on the brain circuits in fear and anxiety have shown that the limbic system, and particularly the amygdala, has a critical role in emotional processing, including the acquisition and expression of fear memories (Phelps & LeDoux, 2005), the detection of aversive or ambiguous stimuli (Davis & Whalen, 2001), fear conditioning (LeDoux, 2000), and processing of emotional facial expressions (Phan, Fitzgerald, Nathan, & Tancer, 2006; Stein, 2002), even in the absence of explicit knowledge that such stimuli were presented (Whalen et al., 1998). It has been shown that the amygdalar-ventral striatal circuitry is important for the association of complex sensory stimuli with positive and negative rewards (Olmos & Heimer, 1999). Other areas involved in the brain circuits of anxiety include the thalamus, which is directly linked to the amygdala and sends the sensory information about anxiety-inducing stimuli, the hippocampus, delivering the contextual information to the amygdala, and an extended prefrontal network, including the

anterior cingulate cortex (ACC), the insula, the orbitofrontal cortex (OFC) and dorsolateral prefrontal cortex (DLPFC), presumably involved in the down-regulation of amygdalar activation and voluntary emotional control (Ochsner & Gross, 2005; Stein et al., 2007).

Within the scope of this thesis, the importance of the limbic-cortical network in SAD will be emphasised and the third chapter will specifically focus on the amygdala, orbitofrontal cortex, and dorsolateral prefrontal cortex as regions of interest. As already mentioned, the aim is to investigate the differences between SAD patients and healthy control participants in amygdalar activation, as well as the role of the prefrontal cortex for emotional down-regulation and the effect that attention plays during emotional processing and cognition. With regard to cognition and attention, certain cognitive models of social anxiety have dominated the scientific scene since the 1990s and will be discussed in some details below.

## *2.2. Cognitive Models of SAD*

As mentioned earlier, cognitive models of SAD suggest the influence of interpretation, memory and attentional cognitive biases that contribute to the maintenance of social anxiety disorder. With regard to interpretation biases, it has been suggested that individuals suffering from SAD tend to interpret neutral facial stimuli as harsh and happy faces as critical, i.e. someone laughing at them (Cooney, Atlas, Joormann, Eugène, & Gotlib, 2006).

In the 1990s, two main cognitive behavioural models of social anxiety have been put forward and have had a significant impact on the research concerning the psychotherapy of SAD. Both the cognitive model proposed by Clark and Wells (1995) and the model by Rapee and Heimberg (1997) are very similar and suggest that

cognitive processes are necessary for the maintenance of social anxiety. The main focus of both theories is on the individual's internal representations during social situations but their views differ with regard to the vigilance for threat in the external environment (Schultz & Heimberg, 2008). While Clark and Wells (1995) suggest that the attention is exclusively self-focused and functions in a closed system of what they call an 'anxiety programme', unable to incorporate new, incoming information, Rapee and Heimberg (1997), while accepting the major role of negative self-imagery, add vigilance to external negative cues as a significant component of SAD.

With regard to memory biases, Rapee and Heimberg's theory (1997) suggests that information judged as threatening would be encoded with a higher reference. Although Clark and Well (1997) agree with the existence of memory biases, their theory suggests that only negative information relevant to the self will be readily encoded, while resources to external information will be limited. To my knowledge, however, there are no conclusive empirical results supporting Clark and Well's claim that attention is only limited to negative self-imagery, without vigilance to negative external stimuli. In a study focusing on memory for social interactions, SAD participants performed better in remembering negative self-related information than recalling partner-related details (Mellings & Alden, 2000). Although the results clearly show a preference for negative self-related information, this does not imply that negative external stimuli are not attended to.

Clearly, individuals suffering from social phobia hold dysfunctional beliefs about themselves and how they are perceived by others, which lead to maladaptive behaviours (e.g. avoidance of social situations due to biased expectations about catastrophic outcomes). In his cognitive theory, Beck (1985) introduces the concept of 'schema', which is a stable structure of beliefs about oneself, others and the world

that is activated in the presence of threat (e.g. a social situation) and influences the individual's perception, interpretation, memory, and behaviour.

Beck's schema is also a core component of the three-stage information processing model of anxiety (Beck & Clark, 1997). According to this model, the first processing stage called initial registration activates an orienting mode in which a stimulus (e.g. emotional face) is automatically evaluated as either being threatening or not. The orienting mode in individuals with SAD is biased and leads to preferential processing of negative cues and misinterpretation of neutral or positive stimuli. The second stage called immediate preparation relies on the activation of schemata. This stage activates the so-called primal mode and aims at minimising danger and maximising survival. It is a combination of automatic (e.g. physiological responses) and strategic (cognitive and behavioural responses) processes and results in hyper-vigilance to threat and automatic negative thoughts. The final, secondary elaboration, stage is completely conscious, activates the meta-cognitive mode and involves strategic processing. According to Beck and Clark (1997), cognitive therapies for SAD should aim at modifying the last stage, as it involves conscious cognitive appraisal.

The three-stage information processing model of anxiety can be understood in two ways. On the one hand, if it is assumed that the model has a linear character, then it can be argued that the initial registration stage, since it is automatic, does not require cognition. This assumption is also in accordance to the affective primacy hypothesis proposed by Zajonc (1980), mentioned earlier in this thesis. On the other hand, however, Beck and Clark's model can also be compared to LeDoux's (1984) two-pathway model of processing, as there are clearly two main components present in both models – bottom-up (automatic) and top-down (conscious) processing modes.

Given the complexity of emotions and SAD in particular and the presumably distributed nature of the brain circuitry, it seems more plausible to assume that the processing network consists of bottom-up and top-down processes that do not exclude each other and may occur simultaneously.

## *2.3. Summary*

To summarise, social anxiety disorder is one of the most common psychiatric conditions. Individuals with SAD suffer from intense dread of social situations and of other people's scrutiny. As a consequence, their condition has an essential negative impact on their quality of life and personal health and well-being. Undoubtedly, recent scientific research has facilitated a better understanding of the neurobiological mechanisms behind SAD and formal models of emotions have identified that cognition is an integral part of affective processing. Cognitive models of anxiety further recognise the important role of cognitive biases and have dominated the recent empirical work on SAD.

Based on the neurobiological and cognitive models discussed in this chapter, the fMRI study included at the end of the thesis will focus on the role of the amygdalar-prefrontal network for the affective processing in SAD. This network involves the amygdala, which is active in response to threat cues, as well as to ambiguous stimuli, and the prefrontal regions responsible for the regulation of amygdala activity (Ochsner & Gross, 2005; Phillips, Ladouceur, & Drevets, 2008). Furthermore, the fMRI study will investigate the effects that attentional processes have on goal-directed cognitive tasks by using an emotional Stroop task paradigm.

Before continuing with the above-mentioned empirical study, the basic principles of (functional) MRI will be discussed in some details in the following chapter.

# III. Methodology

This part of the thesis offers a brief introduction into the methodology used within the experimental study described in the next chapter. It deals with the basic terminology within the realm of functional magnetic resonance imaging (fMRI) and aims at offering a concise overview to beginners with no previous knowledge in the field. The following sections will mainly be based on Lazar (2008), as well as Deichmann (2009) and Poldrack et al. (2011). For a more detailed overview, readers may want to consult Buxton (2003), Faro and Mohamed (2006, 2010), and (Liang & Lauterbur, 2000).

## *3.1. Physics of NMR*

Nuclear magnetic resonance (NMR) imaging is a non-invasive imaging method which relies on the principles of the nuclear magnetic resonance, a physical phenomenon of the nuclear magnetic momentum first described in 1983 (Rabi, Zacharias, Millman, & Kusch, 1938). Due to the negative connotation of the word ‘nuclear’, nowadays this word is omitted and the literature refers to MRI, instead. The first MR images were acquired in 1973 and it took almost a decade until the method was employed to study brain function (Lautenbur, 1973).

In order to understand how (functional) MRI works, some concepts of the physics of nuclear magnetic resonance need to be explained first.

### 3.1.1. Nuclear Spin and External Magnetic Field

Brain tissue consists of atoms, which are made up of protons, electrons and neutrons. Each atom is characterised by its atomic number, which represents the amount of protons, and its atomic weight, corresponding to the sum of protons and

neutrons. Atomic number and atomic weight determine the spin of the atomic nucleus (the centre of an atom, consisting of protons and neutrons), i.e. the rotation around its own axis. Every nucleus with either an odd atomic number or an odd atomic weight has a net spin. If a nucleus has an odd atomic number and an even atomic weight, then the spin is an integer (1, 2, 3, etc.) and if the atomic number is even and the atomic weight - odd, then the spin is of half-integral value (1/2, 2/2, 3/2, etc.) (Lazar, 2008).

Every nucleus with a non-zero spin has a magnetic dipole moment, which can be thought of as an electric current producing a magnetic field. The relationship between the spin (aka. orbital angular momentum) and the magnetic dipole moment of a nucleus is characterised by the gyromagnetic ratio $\gamma$, which is constant for each isotope. In practice, functional magnetic resonance imaging (fMRI) studies the $^{1}H$ isotope of hydrogen (protium) [5], which consists of only a single proton and has the relatively high gyromagnetic ratio of 42.58 MHz/T [6] (Lazar, 2008). It is the most abundant element in the human body and is used for functional MRI of the human brain.

Without any external magnetic field, nuclei with spin, which naturally rotate (or *precess)*, are oriented in random directions, leading to a zero net magnetisation, i.e. $M = 0$ (Lazar, 2008). However, when an object is placed in a magnetic field of strength $B_0$ (e.g. an MR scanner), the spins will align in one of two directions: parallel to the magnetic field (low energy state) or anti-parallel to the field (high energy state), which is a phenomenon called the Zeeman splitting effect. As more spins are oriented parallel to the magnetic field, a net magnetisation $M$ is formed. The number of protons in the high energy state can be increased either through a decrease in

[5] Other isotopes of hydrogen, such as deuterium and tritium, do possess neutrons.
[6] T stands for Tesla

temperature, which is not convenient for most in-vivo NMR-based applications, or by increasing the strength of the magnetic field.

### 3.1.2. Excitation and Relaxation

The magnetisation *M* can be regarded as a vector with a direction and a magnitude (frequency). The direction can be longitudinal, i.e. aligned in the direction of the magnetic field (*z*-axis), and transverse, i.e. aligned orthogonal to the field (in the (*x,y*)-plane) (Lazar, 2008). The precession of the atomic nuclei around the external magnetic field $B_0$ is called Larmor precession and its natural resonance frequency $\omega$ (aka. Larmor frequency) depends on the gyromagnetic ratio $\gamma$ of the nucleus. The frequency is proportional to the magnetic field and can be described as: $\omega = \gamma.B_0$ (Larmor equation).

While the spins are aligned to the z-axis (parallel to the magnetic field), each nucleus rotates at a different phase on the (x,y)-plane, leading to a zero net magnetisation in the transverse direction. This difference in phase is caused by the slight variations in precessional frequencies due to magnetic field inhomogeneities, among other factors. The magnetisation M is called longitudinal magnetisation and is not applicable for fMRI.

However, phase coherence of the spins can be achieved by applying a magnetic field B1 in the plane perpendicular to $B_0$, which causes M to spiral away from $B_0$. This perpendicular flip is also called a 90-degree flip angle. However, in order to achieve excitation, $B_1$ should rotate at the right resonance frequency (equal to the Larmor frequency). Consequently, some of the spins at the lower energy level absorb the applied energy and migrate to the higher energy level. This affects the net magnetisation, which is tilted towards the (x,y)-plane. In other words, the longitudinal magnetisation ($M_z$) is converted into a transverse one ($M_{x,y}$) and $M_z$ is zero.

In absence of an external $B_1$, spin excitation (resonance) diminishes and spins return to their thermodynamic equilibrium (a process known as relaxation). During relaxation, a radio frequency signal is emitted, which can be measured with a receiver coil in the MR scanner. However, with $B_1$ turned off, the spins return 'freely' to their previous way of precessing and the signal decays. This phenomenon is called free induction decay, or FID, and the related relaxation time is called $T_2$* (see the explanation below).

There are different types of relaxation phenomena. For instance, the longitudinal relaxation $T_1$ (or spin-lattice relaxation) refers to the increase of the longitudinal magnetisation from zero during excitation to its normal level at equilibrium. The transverse relaxation $T_2$ (or spin-spin relaxation), on the other hand, causes the transverse magnetisation $M_{(x,y)}$ at the (x,y)-plane to diminish due to the spin dephasing when the external magnetic field $B_1$ is absent. The transverse relaxation is also influenced and accelerated by a number of factors, such as magnetic field inhomogeneities, magnetic susceptibility[7], and chemical shift effects. The relaxation taking all these factors into account is the $T_2$* (or T2-star) relaxation and causes the loss of NMR signal. In contrast to $T_2$*, $T_2$ relaxation considers the internal spin effects only. $T_1$ and $T_2$ occur simultaneously and the relaxation times vary among the different tissues, which allows for the acquisition of contrast in MR images necessary for the differentiation and identification of different brain tissues.

[7] This term refers to the degree of magnetisation of a material in response to a magnetic field. The magnetic field M is strengthened by paramagnetic materials, whereas diamagnetic ones weaken M.

### 3.1.3. Spin Echo

To enable the measurement of transverse magnetisation effects ($T_2$), a special 180°-pulse can be applied, which inverses (or flips) the magnetisation and partially compensates for the spin dephasing effects. This compensation occurs because, in the inversed magnetisation, the 180°-pulse rotates the proton spins to the opposite axis and, therefore, the slower spins come ahead of the faster spins and the latter, due to their higher speed, eventually catch up with the former. This rotation allows the spins to rephrase and form an echo (aka. Hahn spin echo). Consequently, this enables the measurement of an accurate $T_2$ echo, while at the same time the impact of $T_2$* relaxation is limited.

The time between the peak of the 90°-pulse and the peak of an echo is called echo time (TE). Pulses can be applied repeatedly in a certain pulse sequence. The time for which a time sequence is completed once is called repetition time (TR). TE and TR are of essential importance in the process of MR image acquisition.

### 3.1.4. Magnetic Field Gradients

To allow for spatial localisation of the acquired MR signal, a position-dependent magnetic field gradient is applied. With the help of a gradient coil, the strength of the external magnetic field $B_1$ can be varied, which will allow the distinction among different resonance frequencies associated with different locations in the brain (Lazar, 2008; Deichmann, 2009). The gradient pulses can be applied in the three possible directions (along the x-, y-, and z-axes) and are denoted by $G_x$, $G_y$, and $G_z$. There are three types of magnetic field gradients that can be applied in MRI: slice selection, frequency encoding, and phase encoding. Their properties are similar but the timing and direction of their application vary.

A slice selection gradient ($G_{ss}$ [8]) is applied perpendicular to the selected slice plane (for example, $G_z$ for axial slices) at the same time as the 90°-RF pulse is applied to $B_0$ (see the explanation of $B_0$ and $B_1$ in 3.1.2 above). The $G_{ss}$ shifts the net magnetisation M of the nuclei in the desired plane. This shift, however, does not deliver any spatial information if magnetic field gradients are not applied to the other two directions, e.g. along the (xy)-plane for axial slices. Slice selection, together with the transmitted RF bandwidth (the range of frequencies in the slice selection) and the gyromagnetic ratio, determine how thick the slices will be. Slice thickness can be increased by increasing the RF bandwidth or by decreasing the gradient $G_{ss}$.

To better understand how the localisation works, Lazar (2008) suggests the representation of the tissue in a selected slice as being divided into an array with rows and columns. First, a phase-encoding gradient $G_{pe}$ is applied to the nuclei rotating in phase (after excitation and before the subsequent frequency-encoding gradient $G_{fe}$) for a limited time period. This $G_y$ gradient modifies the spin resonance frequencies, causing all the nuclei to precess with the same frequency, but different phases. Referring back to the array, nuclei on different rows precess at slightly different phases, but within the row, the same nuclei are still precessing in phase (Lazar, 2008).

During data acquisition, the frequency-encoding gradient $G_{fe}$ (aka. readout gradient) is applied, which causes the external magnetic field to increase linearly in the x-direction. This $G_x$ gradient causes the nuclei in different columns of the array to precess at different frequencies, while within a column the frequency of precession is constant.

[8] SS stands for slice selection.

All in all, within the array defined by a certain slice, each location has distinct phase and frequency and in this way elements can be distinguished from each other.

### 3.1.5. Gradient (Recalled) Echo (GRE, GE)

The application of magnetic field gradients discussed above poses some issues concerning the acquisition of a signal. Specifically, the above-mentioned shift in magnetisation due to the gradients obviously results in inhomogeneities of the static magnetic field, which in turn accelerates the signal decay (FID) (Deichmann, 2009). To recall, the frequency-encoding gradient causes spins to precess with different Larmor frequencies. Consequently, after a while, the spins are completely dephased and their magnetisation vectors cancel each other out.

The solution to this problem is to reverse the gradient polarity after a predetermined time period, which is achieved by applying a dephasing gradient before the frequency-encoding (readout) gradient. Due to the inversion, the spins turn backwards, maintaining their frequencies, which results in rephrasing of the spins (Deichmann, 2009). In other words, the gradient recalled echo is produced by deliberately applying a gradient of one polarity to dephase the transverse magnetisation spins and then using a gradient with the opposite polarity to rephrase the spins. The rephrasing effect occurs when the readout is stable, permitting the measurement of a stronger signal.

The essential difference between gradient echoes and spin echoes is that the former do not require a second 180°-RF pulse, but rather only one RF-pulse. This leads to shorter repetition times (TR) and in turn allows for increased imaging speed. However, since the dephasing and rephrasing occur in the same direction as the main magnetic field, the $T_2$* effects are not excluded, as in the case of applying a

180°-RF pulse. Hence, the GRE is more sensitive to magnetic field inhomogeneities, magnetic susceptibility, and chemical shift effects.

Additionally, while spin echoes use a 90°-RF pulse, in the case of GRE, the flip angle can vary and is usually below 90°. This is referred to as a partial flip angle and results in decreased transverse magnetisation $M_{(x,y)}$. When the $M_{(x,y)}$ is lower, the thermal equilibrium (the return to $M_z$) will occur faster, allowing shorter TR and TE and also shorter scan time. In general, gradient echo TRs and TEs are shorter than those of spin echo pulse sequences. The choice of an optimal flip angle and the manipulation of TR and TE are crucial for the acquisition of reliable data.

### 3.1.6. *k*-Space and Single-Shot Echo Planar Imaging

*k*-space, a mathematical concept developed by Twieg (1983) and Ljunggren (1983) independently, is significantly valuable for a more simplistic explanation of the MR signal acquisition.

Previously, the localisation of the magnetic resonance signal was discussed in the context of field gradients. The magnetic resonance signal is composed of a series of sine waves with their individual frequency and amplitude. The signal is encoded into a Fourier frequency-phase domain, or *k*-space. As discussed earlier, a selected slice can be represented in terms of an array with an *x*- and *y*-axis. To recall, the *x*-axis corresponds to the frequency-encoding gradient $G_x$, while the *y*-axis – to the phase-encoding gradient $G_y$ during axial slice acquisition. The signal obtained with no $G_y$ is located in the centre of the *k*-space. Moving along the *y*-axis causes $G_y$ to increase. By applying the frequency-encoding gradient $G_x$, a row in the *k*-space is sampled for a given phase (Lazar, 2008).

Generally, *k*-space is an array of numbers with the most essential data in the centre of it. However, this is not to say that only the centre is important for the

acquisition of data. It simply contains the low frequency information that determines the contrast in the image, while the details are stored in the edges and lines. Each array represents the raw data space and every point in the *k*-space corresponds to a wave in the image with a different spatial frequency and a different angle, i.e. a point with its own $k_x$ and $k_y$ value. In order to obtain an image, the raw data stored in the *k*-space needs to be digitised using Fourier transformation, which separates the frequencies of a signal and makes it possible to identify the amplitude of signals produced at different frequencies. A point in the raw data matrix (*k*-space) does not correspond to a point in the obtained MR image because each point in the matrix contains part of the information for the whole image.

However, if a separate RF-pulse is used for each point in the raw data matrix, *k*-space data acquisition will demand enormous amount of time. Single-shot echo planar imaging enables the acquisition of many echoes after a single RF-pulse. Fast-switching gradients periodically turn on and off to generate a series of gradient echoes. All k-space lines are measured in one TR (repetition time). For fMRI, TRs typically lie within 1 to 3 sec. for whole-brain coverage, which determines the spatial resolution of the data. The first echo is placed at the edge of *k*-space by a large phase encoding gradient $G_{pe}$. The readout gradient $G_{fe}$ generates a train of echoes along the lines of the *k*-space. The jumps from one line to the next are facilitated by short $G_{pe}$ blips (Lazar, 2008).

Single-shot EPI allows for fast scanning time and reduced motion artefact effects and is a powerful imaging technique for functional localisation at the cost of reduced tissue contrast and image distortions. After the image acquisition, the fMRI images can be co-registered and underlayed with high-resolution anatomical images

of the individual or standard brain templates to complement the functional findings with anatomical details.

### 3.1.7. MR Image Acquisition Parameters

The magnetic field gradients determine the way the *k*-space is sampled, as well as the resolution and the field of view (FOV). FOV is defined as the physical size of an image and is measured in $mm^3$. It specifies the regions from which the image is sampled. FOV, together with the acquisition matrix size[9], determine the two dimensions of a voxel [10] in the plane of a slice (Lazar, 2008). If more tissue needs to be imaged (a greater FOV), the likelihood of magnetic field inhomogeneities increases and leads to lower effective resolution of the image, under the assumption of constant matrix size. However, a smaller FOV leads to a smaller voxel size and higher resolution but for the expense of a reduced signal-to-noise ratio (SNR).

The quality of an image is influenced by unavoidable noise introduced in the data (e.g. due to the inherent thermal noise of the spin system, body movement during scanning, MR artefacts resulting from differences in magnetic susceptibilities, etc.). Noise can be seen as an additional fluctuation of a signal which does not carry any image information. The relationship between MR signal intensity and noise is represented by the signal-to-noise ratio (SNR).

SNR is influenced by a number of factors, such as voxel size, the number of phase encoding steps Ny, the number of excitations (NEX)11, and RF-bandwidth, among others (Lazar, 2008). First, greater voxel size will increase the amount of excited nuclei, leading to a stronger MR signal and therefore a higher SNR (but for

[9] This is size of the grid (usually in the form of a square) into which the plane of the FOV is divided for each slice (Lazar, 2008).
[10] Voxel stands for *volumetric pixel* and is the basic sampling unit of MRI.
[11] NEX is the number of times a scan is repeated.

the expense of degraded spatial resolution, as mentioned earlier). Second, Ny and NEX also cause SNR to increase, following a square root law: doubled Ny and NEX increase SNR by a factor of √2. And finally, a larger RF-bandwidth will increase noise, influencing the SNR negatively (Lazar 2008). Other factors playing a role in the image acquisition processed are echo time (TE) and repetition time (TR). TE and TR can be manipulated to weight MR images, for example towards T1 relaxation, T2 relaxation, or T2* relaxation. To recall, different tissues have different T1 and T2 relaxation times. For instance, ventricular and grey matter areas appear dark in T1-weighted and bight in T2*-weighed images (see Figure 1). Furthermore, T2*-weighted functional EPI images are often distorted in frontal brain areas as a result of local magnetic field inhomogeneities caused by tissue inhomogeneities and air cavities.

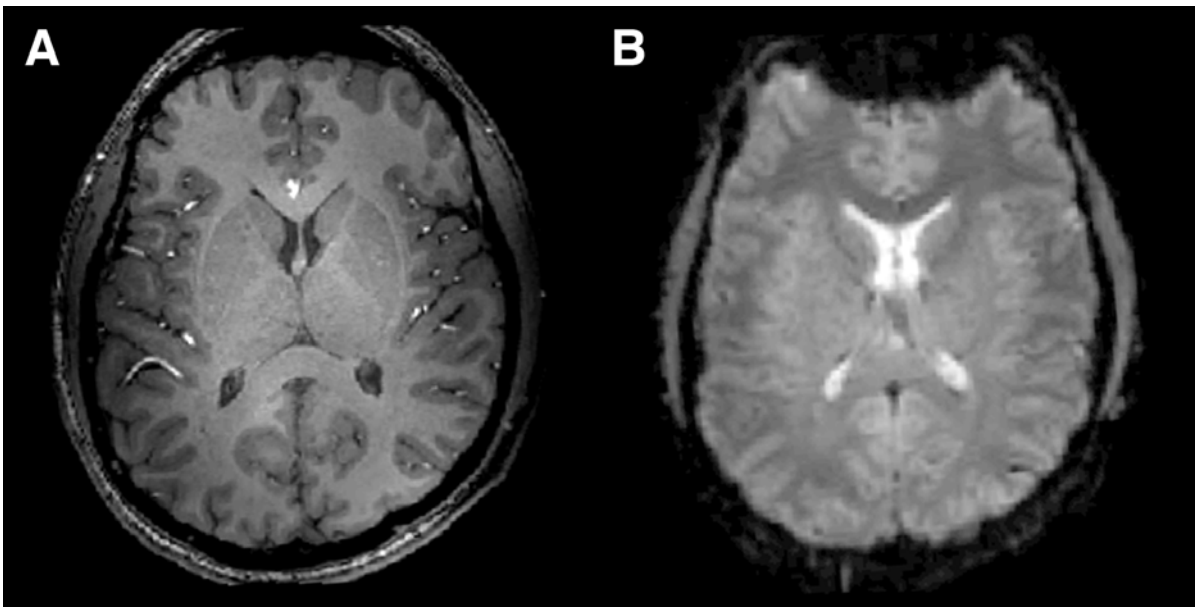


Figure 1. Brain images acquired at 7T.
*A. T1-weighted anatomical image. B. T2*-weighted EPI image.*
*Courtesy to Ronald Sladky for providing the images*

$T_1$-weighted images offer good contrast between grey and white matter in the brain. They depict differences in $T_1$ relaxation time of various types of tissue and are

acquired by using spin echo sequences or GRE sequences. To produce $T_1$-weighted images, short TR and short TE are required. In contrast, $T_2$-weighted images are spin-echo-based and are acquired with long TR and long TE. Similarly to T1-weighted images, they differentiate between fat and water, although the contrast will be inverse, with water (e.g. cerebrospinal fluid) appearing lighter and fat - darker. Generally, $T_2$ contrasts have found wide application in pathological diagnosis. $T_2$*-weighted scans are acquired using GRE sequence, with long TE and long TR. Despite their proneness to $T_2$* relaxation effects, they have the advantage of increasing contrast for certain types of tissue (e.g. venous blood).

All in all, the acquisition of MR images always faces some trade-offs and the best solution depends on the adequate manipulation of the parameters discussed above and the goals of the researcher. The following chapter will focus on the basic principles of functional magnetic resonance imaging (fMRI).

## *3.2. Basics of BOLD fMRI*

BOLD fMRI stands for blood oxygenation level-dependent functional magnetic resonance imaging (hereafter: fMRI[12]) and relies on the principles of MRI and the fact that oxygenated and deoxygenated haemoglobin introduce different susceptibility effects. fMRI measures brain activity by detecting the haemodynamic response of the brain, i.e. changes in blood flow and blood oxygenation level during activation. Most importantly, fMRI is an indirect measurement tool, as it does not detect the activation itself, but the metabolic changes resulting from the brain activity. Specifically, when neurons in the brain become active, they require more glucose and therefore more oxygen-rich blood flows through the activated area (Poldrack, Mumford, & Nichols,

[12] There are different forms of fMRI, although the term is often used to refer to the most commonly used one, which employs BOLD contrasts.

2011). This principle will be discussed in more detail below. In addition to the physiological principles of BOLD fMRI, this chapter will also focus on experimental design, data preprocessing, and data analysis.

### 3.2.1. Basic Physiology of BOLD fMRI

The properties of haemoglobin are essential for the application of fMRI. Haemoglobin is a protein found in the red blood cells, responsible for the transportation of oxygen from the lungs to the brain (as well as other tissues of the body). It comprises four globin chains, each containing a so-called heme group. There exists an iron atom[13] in the centre of each heme group and an oxygen atom can be attached to the group. Oxygen-bound haemoglobin, oxyhaemoglobin ($HbO_2$), is diamagnetic and has little effect on the magnetic field, whereas deoxyhaemoglobin (dHb), which has no bound oxygen molecules, is paramagnetic and creates distortions to the external magnetic field of the MR scanner. As discussed earlier, magnetic field inhomogeneities cause the phase coherence of the hydrogen protons to decrease, which in turn leads to a loss of overall signal and is directly linked to $T_2$* relaxation effects. However, when regions are activated, the oxygenation level is enhanced, resulting in a stronger MR signal. Due to the dependence of BOLD effect on $T_2$* relaxation effects, echo times (TE) need to be carefully chosen. If the TE are too short, the BOLD sensitivity will be low, with almost no $T_2$* weighting possible. On the other hand, too long TE will lead to faster signal decays, as already discussed earlier. Basically, maximum BOLD sensitivity is accomplished at TE equal to $T_2$*, or at around 45 ms at 3T scanner (Deichmann, 2009).

The explanation of the BOLD effect as an interplay between dHb and $HbO_2$ is relatively simplified. In fact, there are more complex processes involved, which are

[13] Elementary iron has diamagnetic properties.

still not fully understood. For instance, oxygenated haemoglobin is influenced by factors such as regional cerebral blood flow (rCBF), cerebral blood volume (CBV), and cerebral metabolic rate of oxygen ($CMRO_2$). Also, BOLD contrast is sensitive to venous changes because the difference between oxygenation and deoxygenation states there is greater, which can create spatial distortions of the signal acquired. These issues will be discussed in more detail in the next section.

### 3.2.2. Haemodynamic response

As mentioned earlier, the haemodynamic response measures metabolic changes, thus, only indirectly estimating neuronal activity. When the brain is activated, the local energy demand also increases. As a result from neuronal firing, the neurotransmitter glutamate is released, which influences the calcium ion concentration in the astrocytes, star-shaped glial cells highly abundant in the human brain. In turn, the high $Ca^+$ concentration in the astrocytes causes the release of nitric oxide (NO) in the arterioles (medium-sized blood vessels connecting the arteries with the capillaries). Due to the vasodilating properties of NO, the arterioles are expanded and enable the supply of more blood (Ogawa & Sung, 2007).

Regional CBF increases in order to deliver the necessary oxygen and glucose to the brain, leading to a higher level of $HbO_2$. At the same time, $CMRO_2$ also rises and consequently more oxygen is consumed, enhancing the concentration of dHb and reducing the BOLD effect (Deichmann, 2009). However, the rCBF outpaces the metabolic rate of oxygen, resulting in hyper-oxygenation and therefore to enhanced MR signal during activation.

Due to the elasticity of the vascular tissue of the veins and venules, higher rCBF leads to an increase in CBV (Glaser, Friston, Mechelli, Turner, & Price, 2004), although the dynamics of CBV does not match the dynamics of rCBF. When blood

volume increases, so do $HbO_{2,}$ as well as deoxyhaemoglobin (dHb) concentration (Buxton, Wong, & Frank, 1998). Considering the space constraints imposed on the human brain, it is clear that an increase in blood flow requires complex regulating mechanisms. Generally, oxyhaemoglobin is supplied to the brain by the vascular arterial system and the oxygen-depleted blood is drained through the venous system.

Clearly, significant CBV changes can be observed primarily in the venous system due to the size of their vessels and their elastic properties mentioned above (Buxton et al., 1998). According to the Balloon model proposed by Buxton and colleagues (1998), the increase in rCBF causes the inflation of a venous ‘balloon’, enabling deoxygenated blood to be diluted and expelled at a greater rate (Glaser et al., 2004). Consequently, the level of deoxyhaemoglobin is reduced, enhancing the MR signal. However, the sensitivity of the BOLD signal to venous changes needs to be suppressed in order to ensure a better spatial resolution. This can be achieved by using multiple gradient echo sequences or spin echo sequences. Alternatively, stronger static magnetic fields can also help eliminate the signal from larger draining veins.

In a nutshell, the haemodynamic response illustrates the metabolic changes that occur during brain activation. The BOLD contrast is the result of the decrease in levels of deoxyhaemoglobin of certain brain areas during activation relative to a baseline state and is strongly modulated by the dynamics of CBF, $CMRO_2$ and CBV responses. Typically, the haemodynamic response occurs 1-2 sec. after the actual neuronal activity and the response peak is observed at approx. 5 sec. after stimulation, followed by an undershoot lasting approx. 30 sec (Figure 2).

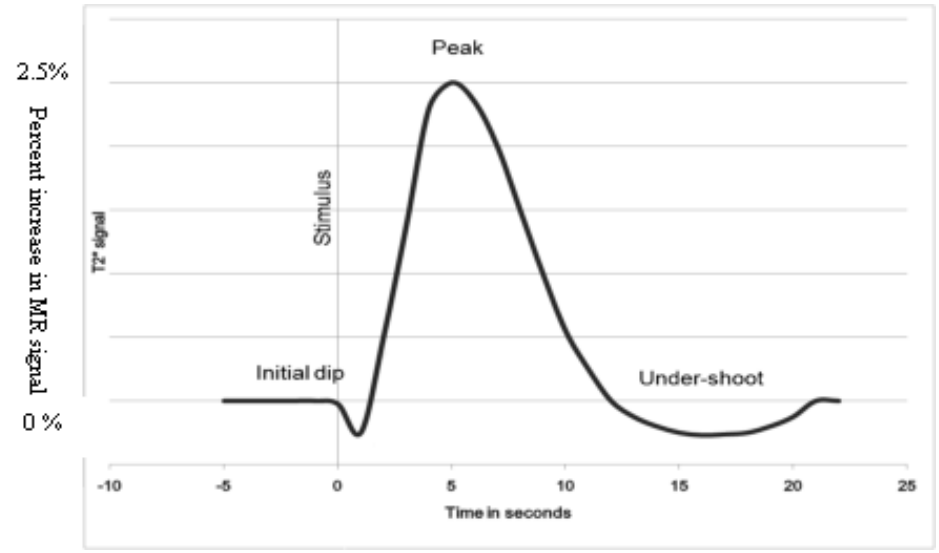


Figure 2. The hemodynamic response function
*Source: http://radiopaedia.org*

The hemodynamic response function can be described as follows: An initial dip is sometimes observed at the beginning (especially at high magnetic fields), although there is a lack of plausible explanation for and convincing replication of this phenomenon. Then, a rise of the signal occurs, resulting from the increase in rCBF due to the vasodilation of arterioles, and reaching a peak, or an overshoot, resulting from the over-compensatory response outpacing the $CMRO_2$. If no activation is maintained, relaxation of rCBF and CBV occurs, resulting in a decrease of MR signal. Before the return to baseline, a post-stimulus undershoot is usually observed, which can be explained by the slower relaxation time of CBV relative to rCBF.

Among the main problems that haemodynamic response (HDR) analysis faces are the variability and difference in amplitude in the observed response, which can occur not only among participants, but also within a single participant following multiple scans and even within different brain regions of the same participant. In addition, the delay in the HDR leads to a relatively poor temporal resolution. Other issues deal with the ongoing debate regarding the physiological basis of the BOLD

signal and the plausibility of data interpretation with respect to measuring neural activity (Logothetis, 2002). For a more detailed discussion of these issues, which is unfortunately beyond the scope of this thesis, readers can refer to Arthurs & Boniface, 2002, as well as to Logothetis, 2002 and Glaser et al., 2004.

### 3.2.3. fMRI Experimental Design

Depending on what fMRI experimental design is applied, the BOLD response can arise from an impulsive neural activity (an event) or from an activity that is sustained for several seconds after stimulation (an epoch) (Henson, 2004). With respect to stimulus presentation, there is a generally accepted differentiation among three main types of fMRI experimental design: block (or epoch), event-related, and mixed. It was the block design that was traditionally used in fMRI experiments due to its statistical power and relative independency on how the haemodynamic response is modelled. In fact, all types of fMRI design have their strengths and weaknesses, as will be discussed below.

#### *3.2.3.1. Block design*

In a block (or boxcar[14]) design, blocks are shown for a fixed length of time and each block comprises one type of stimulus presentation (Lazar, 2008). A common paradigm is the alternation between blocks of stimulation, in which one condition is presented for a fixed period of time (e.g. 16 sec.), and blocks without stimulation (rest or fixation). An alternative block design can be used to study the difference between two similar conditions A and B by switching between blocks comprising condition A and blocks consisting of condition B. In this case, however, the activity common to both A and B cannot be identified. In order to detect signal difference against

[14] The term *boxcar* originates from the „on-off"-nature of the block design.

background noise, the conditions which need to be contrasted should not lie far apart in time (Henson, 2007).

Basically, block designs rely on the assumption that successive responses add in a linear fashion and if the activation is sustained, the HRF can reach maximal values and then return to baseline during non-stimulation. The main advantage of the block design is its statistical power and its suitability for experiments in an early, exploratory stage. Block designs allow for assessing BOLD signal magnitude differences between conditions but are to a lesser degree suitable for characterising the haemodynamic response function (no separation of responses to individual trials are possible).

One of the disadvantages the block design faces is that the choice of a baseline condition can be problematic due to the inability to control the resting condition (i.e. effects of other processes, such as day dreaming or emotional processes cannot be excluded). Additionally, although the neural processes throughout the same trials should presumably be the same, in fact, anticipatory effects concerning the order and duration of blocks can lead to difference in the activation of initial trails relative to later ones. Also, the block design is inappropriate for studying certain cognitive tasks (e.g. oddball paradigm used for studying a reaction to an unexpected stimulus).

#### *3.2.3.2. Event-related design*

In contrast to block designs, event-related designs offer a higher experimental flexibility, since stimulus events from various conditions can be presented randomly in one run. The randomisation of trials allows the avoidance of anticipatory and habituation effects. The response to each individual trial, rather than a block of trials, can be examined by identifying the HRF from each event type. This allows for better

temporal resolution and an identification of change over time, but requires a more complex statistical analysis and relies on the adequate HRF modelling.

Each event is separated by an inter-stimulus interval (ISI), which can be varied, resulting in the differentiation between slow and rapid event-related designs. Generally, the BOLD response occurs with a delay relative to the stimulus duration. When stimuli are spaced close to each other (the case of rapid event-related designs) the post-stimulus delay of the BOLD signal will cause the HRF to overlap. In order to analyse the haemodynamic response to each trial, deconvolution techniques for disentangling the HRF are required.

Slow event-related designs use long ISI to prevent the overlap of the HRF and allows for a simpler statistical analysis. A main disadvantage is that slow event-related designs are obviously time-consuming. Since event-related designs, in general, have low signal-to-noise ratio (SNR), a higher number of trials per condition is recommended. If long ISI are applied, this will result in longer scanning times. Moreover, long ISI can negatively influence the motivation of the participant and cause anticipatory effects.

In addition to the alternation between ISI and events, ISI duration can also be divided into fixed or jittered. An example of a jittered ISI is the self-paced response to stimuli, in which the individual decides on when the next stimulus will be presented. This allows for more randomness and unpredictability, which decreases the anticipatory effects and increases the sampling performance of the HRF, but is more challenging for analysis. Similarly, mixed designs can be used to study the inter-relationships between emotional states (i.e. sustained process) and the processing of a discrete trial (e.g. detection of a fearful face) (Garavan & Murphy, 2009).

*3.2.3.3. Mixed design*

Mixed designs combine features from both even-related and block designs and enable the analysis of sustained (task-related) processes, as well as transient (trial-related) responses (Petersen & Dubis, 2012). It was shown that sustained responses can be elicited even when a given task is not performed but only attended to (e.g. visually-evoked responses), suggesting the influence of top-down (attentional) processes (Chawla, Rees, & Friston, 1999).

The application of a mixed design needs a careful consideration of a number of factors. For example, poorly designed experiments may result in misattribution of signals from one type of processing to the other, which will have a negative impact on the acquired results and the subsequent conclusions (Petersen & Dubis, 2012). Additionally, in contrast to block or event-related designs, recruiting a higher number of participants is recommended to ensure statistical strength of sustained effects. Obviously, mixed design would require a more complex statistical analysis and is more prone to errors, but at the same time, if applied correctly, can deliver useful and interesting results.

### 3.2.4. fMRI Data Preprocessing

Raw fMRI data are biased by a lot of noise arising from different sources: thermal noise, system noise, and subject-related noise (Lazar, 2008). Therefore, a number of preprocessing steps are necessary in order to prepare the data for statistical analysis. This section deals with the types of noise typically present in the raw fMRI data and the most widely used preprocessing steps prior to data analysis.

*3.2.4.1. Origin of noise*

Thermal noise is caused by thermal motion of electrons in both the participant and the scanner over time and leads to fluctuations in the MR signal intensity (Lindquist, 2008). The thermal noise increases with an increase in temperature, as well as at higher magnetic fields. However, it is generally Gaussian-distributed and independent of the experimental task. Its undesired artefactual influence on the analysis efficacy can be mitigated by the employment of spatial smoothing (Lazar, 2008).

System noise originates from the MR scanner itself resulting from inhomogeneities in the static magnetic field and instabilities in the gradient fields. Scanner instabilities can cause scanner drift resulting in gradual and systematic change in voxel intensity over the course of scanning. Spikes, another example of scanner artefacts, are brief changes in brightness due to electrical instability in the scanner, which appear as a regular pattern of stripes across the acquired image (Poldrack et al., 2011). Ghost artefacts (aka. EPI Nyquist ghost) are due to a slight offset in phase between different lines of *k*-space in the EPI acquisition, which can occur as a result of instability in the gradient coils, but can also result from subject movement or physiological noise, such as respiration. As a consequence, the artefactual convolution of the acquired MR signals in k-space can lead to improper spatial mapping (ghost images).

Physiological artefacts fall within the category of subject-related noise. For instance, heartbeat and respiration lead to signal fluctuations that are periodic and difficult to model. A major source of noise in the fMRI data is motion, especially head motion, leading to signal blurring. Specifically, the activation from one location is contaminated with activation from nearby locations and even small amounts of movement can have a very negative impact on the acquired data when correlated to

the time course of the fMRI task (Lazar, 2008). Another source of subject-related noise has its origin in the fact that the human brain is always active. Consequently, transient, task-irrelevant responses (e.g. attending to the surrounding, day dreaming, etc) can activate areas outside the regions of interest (ROIs) and hinders the definition of a pure baseline condition in the fMRI paradigm.

*3.2.4.2. Slice timing correction*

Slice acquisition can occur sequentially or in an interleaved fashion (e.g. first even and then odd slices). Commonly, slices are acquired one at a time and not all at once, leading to a time shift in acquisition. Therefore, it is desirable to temporally shift slices according to their acquisition sequence by either using interpolation or the Fourier shift theorem (Lindquist, 2008). A recent analysis of the impact of the slice-timing effect suggested that slice-timing correction methods are highly recommended and are a necessary step in the preprocessing pipeline (Sladky et al., 2011). However, in case there are extensive motion artefacts (e.g. in some neurological or psychiatric patients), the slice-timing correction step should be completed after the motion correction.

*3.2.4.3. Motion correction*

As mentioned earlier, motion artefacts can be a major source of error and should be treated adequately. The first step is to find a target image (usually the first image or the mean image[15]), which is used for the alignment of the input image. The input image is transformed to match the target image by rigid body transformation involving six parameters (three translations, i.e. shifts in the *x*, *y* and *z* directions, and three rotations, i.e. altering roll, pitch, and yaw) (Lindquist, 2008). The matching process

[15] The mean image corresponds to the average of all acquired images.

involves minimising an appropriate cost function[16] (e.g. sums of squared differences, i.e. the average squared difference between voxel intensities in each image). As soon as the optimal realignment parameters are set, the input image is re-sampled using interpolation and a new motion-corrected image is created (Lindquist, 2008). This procedure is applied to all acquired images.

*2.2.4.4. Co-registration and normalisation*

Functional scans have typically low spatial resolution. As a result, co-registration can be applied to overlay functional images onto an average structural image in order to link the functional scans to an anatomical scan. The co-registration process is typically performed by using a rigid body transformation with six parameters (see above). Re-slicing the data is necessary after co-registration, e.g. when the image dimensions are changed. The advantage of co-registration is that it aids in normalisation and allows the display of activation on anatomical images.

The purpose of normalisation is to register each subject's images to a standardised stereotaxic space defined by a template brain (Talairach or MNI[17]) in order to compensate for individual differences. As a result, the normalised images can be compared across different studies and participants (Lindquist, 2008). Normalisation is produced by using non-linear transformations (warping) to match local features.

To increase the efficiency of the normalisation algorithm, segmentation can be used to classify voxels within an image into different anatomical divisions: grey matter, white matter, and cerebrospinal fluid (CSF).

[16] Cost function is a way to define the differences between the two images prior to alignment.
[17] Montreal Neurological Institute

*3.2.4.5. Spatial smoothing*

Spatial smoothing implies that data points are averaged with their neighbouring points. It is generally used to increase SNR and improve inter-subject comparability by averaging out small spatial differences in brain anatomy and functional localisation. Smoothing involves convolving the functional images with a Gaussian kernel, described by the full width of the kernel at half its maximum height (FWHM) (Lindquist, 2008). FWHM is measured in mm and typically has the value of 4-12 mm

Spatial smoothing can be regarded as a low pass filter, blurring sharp edges of an image, but also reducing spatial resolution. Additionally, if the shape and size of the signal is not known, it is a challenge to achieve accurate spatial smoothing (Lazar, 2008).

### 3.2.5. fMRI Data Analysis

fMRI data can be treated as time series due to the fact that the BOLD signal tends to be correlated across successive scans (Henson, 2004). The aim of fMRI data analysis is to observe the time series of each voxel in order to see if there are changes in BOLD signal in response to some experimental manipulation (Poldrack et al., 2011). Statistical analysis is conducted in order to determine which voxels are activated by the experimental task.

*3.2.5.1. General linear model (GLM)*

A most well-established statistical tool in fMRI data analysis is the general linear model (GLM)[18], which aims at predicting the voxels' time series (the dependent variable) in terms of a linear combination of independent variables or different reference functions (aka. regressors, covariates, basis functions, or explanatory

[18] In the context of fMRI analysis, the univariate version of GLM is used (univariate in reference to the number of dependent variables, i.e. each voxel separately).

variables). Reference functions refer to the responses to different stimuli in an fMRI experimental setting. In other words, GLM assumes that each stimulus has its own predicted response and the data measured in each voxel can be explained by the linear combination of these predicted responses (Woolrich, Beckmann, Nichols, & Smith, 2009). The GLM can be described in the following form:

$$Y = X\beta + \varepsilon$$

where *Y* is the measured BOLD signal at various time points at a single voxel, *X* is the design matrix, *ß* (aka. regressor parameter or effect size) represents the parameters that define the contribution of each component of the design matrix to the value of *Y*, and is *ε* the error (the difference between the observed data and the one predicted by the model). The design matrix X consists of multiple columns, each representing a particular experimental condition (i.e. predicted response to a given stimulus) and the rows refer to the different time series. The GLM analysis aims at finding the parameter estimates (*ß*s), representing a set of amplitude values that best fit the data (i.e. minimise the squared error). Parameter estimates *ß* can also be compared with each other by considering their contrasts $c^T\beta$, where *c* is a contrast vector. For instance, the SPM software allows for the consideration of two different types of contrast: F-contrast and T-contrast. While the F-contrast is useful for testing whether there is any significant activation resulting from certain parameters (e.g. task A vs. task B), it cannot tell which parameter (e.g. A or B) is driving the effect. T-contrast, on the other hand, gives information about the direction of an effect and shows which parameter is driving the effect, but it can only test one individual model parameters (e.g. is A greater than B) and not a subset of parameters (e.g. effects of interest).

Contrast vectors enable the estimation of signal magnitudes in reference to one condition or to an average over multiple conditions, as well as the estimation of the difference between two conditions (Lindquist, 2008).

*3.2.5.2. Temporal autocorrelation / non-orthogonality*

It is assumed that the noise ε is unique to each voxel and can be modelled by a Gaussian distribution with a standard deviation (Woolrich, Beckmann, Nichols, & Smith, 2009). In practice, however, the amount of noise at each time point is correlated to the noise at the neighbouring time points. This is called temporal autocorrelation (or non-orthogonality) and can negatively impact the accuracy of the model fitting method and the subsequent statistical analysis. A common way to deal with this problem is by using autoregression (AR) models, which estimate the amount of autocorrelation in the data and remove the noise that is correlated from the signal.

*3.2.5.3. Modelling the HRF*

GLM is a powerful but also a rigid approach to data analysis. It assumes that the stimulus function and the HRF are known, which implies that if any of them is not modelled properly, this will result in severe power loss (Lindquist, 2008). In fact, the haemodynamic response may vary between brain regions and across subjects, as well as within the same subject, which should carefully be considered to avoid mismodelling.

The relationship between the BOLD signal and the neural response to stimulation tends to exhibit linear time invariant (LTI) properties, suggesting that a neural response scaled by a certain factor and shifted by *t* seconds will lead to the same changes in the BOLD signal. Consequently, the predicted BOLD response can be obtained using convolution, which is a way of blending the stimulus onset time

series with an HRF together to create the shape of the BOLD response (Poldrack et al., 2011).

The “canonical” HRF is typically based on the combination of two gamma functions – one modelling the initial stimulus response and the other accounting for the undershoot (Friston, Josephs, Rees, & Turner, 1998). However, if the variability in the HRF across brain regions and subjects is to be considered, a more flexible HRF model is required. For instance, the HRF model can be extended to include more versions of the canonical HRF, also called basis functions (e.g. adding temporal and dispersion derivatives). Another choice is the use of a finite impulse response (FIR) basis set, allowing for the estimation of an arbitrary HRF shape for each event type in every voxel of the brain. This is achieved by choosing a time window around a stimulus and then using GLM to model the response at each time point within the window following stimulation (Poldrack et al., 2011).

However, basis sets, such as FIR, face the so-called bias-variance trade-off. In other words, if too many basis functions are included in a set, this could lead to over-fitting, i.e. less sensibility in distinguishing the genuine signal from the random fluctuations of the fMRI noise. This issue is sometimes overcome by using a Bayesian approach, which allows the inclusion of prior information (Woolrich, Beckmann, Nichols, & Smith, 2009). Basically, FIR is suitable for the estimation of the HRF (characterisation of its shape) and less for detection of activation.

*3.2.5.4. Group analysis*

The statistical modelling described so far refers to single-subject (one-level) analysis. However, group analysis requires treatment of the data as hierarchical and consisting of two levels. On the first level, the data for each subject are modelled separately, including subject-specific estimates and within-subject variance estimates. On the

second level, the input from the first level is used to estimate the between-subject variance (Poldrack et al., 2011).

Group analysis of fMRI data requires a mixed-effect model, which takes fixed and random effects into consideration. Fixed effect analysis assumes that the only source of error is the scan-to-scan variability and error variance is the same for all subjects. However, the inter-subject variance is not accounted for. In an fMRI experiment, a small number of (randomly chosen) participants are assumed to represent a larger population. In order to draw conclusions for the larger population based on the random sample, a random-effects analysis is necessary.

*3.2.5.5. Inference (thresholding) on images*

So far, the steps concerning the specification of the GLM design matrix and the estimation of the GLM parameters have been described. The next step is to use the parameter estimates to create statistical parametric maps (SPMs), based on voxel-wise GLM and Gaussian Random Field (GRF) theory[19]. Specifically, the parameter estimate (PE) is converted into a *T* value, which considers the PE, as well as its standard deviation (or uncertainty in its estimation). In the best case, the T-maps will have zero values if there is no effect and large values in the presence of activation. However, this does not hold true for fMRI data partially due to the noise inherent in the data. Consequently, statistical inference is applied in order to decide which voxels show a signal influenced by the experimental manipulation and which voxels exhibit a signal attributable to noise.

[19] An alternative to SPMs are the posterior parametric maps (PPMs). While SPMs are applied for classical inferences, PPMs make use of Bayesian (or conditional) inferences based on the posterior distribution of the activation given the data and does not require an assumed existence of the null hypothesis Friston (2009).

The traditional univariate statistical inference involves a classical hypothesis testing, comprising a null hypothesis $H_0$ (or the absence of any observable effect), which is taken as the default case, and the alternative hypothesis $H_1$ (or the scientific hypothesis of interest) (Poldrack et al., 2011). In order to reject or accept the $H_0$, p-values are computed from the data. Essentially, the p-value is the probability of observing a signal given that the null hypothesis is true and therefore can only be used to refute the $H_0$, but is unable to show evidence for the existence of the $H_0$.

As mentioned earlier, the fMRI analysis requires the separation of an experimentally relevant signal from a signal caused by noise, which can be achieved by using thresholds. In the case of voxel-wise inference, a threshold $u$ is assigned for an image and only voxels above this significance threshold are considered. Alternatively, cluster-wise inference makes use of a cluster-forming threshold $u_{clus}$ and neighbouring voxels are grouped in clusters. Only those clusters exceeding a significance threshold $k_\alpha$ are marked as significant (Woolrich, Beckmann, Nichols, & Smith, 2009). While voxel-wise inference considers individual voxels and is recommended for detecting focal, intense signals, cluster-wise inference is good for low, spatially extended signals, but cannot tell which voxels within the cluster deliver the signal.

*3.2.5.6. Statistical errors*

Basically, there are two types of errors that can occur during hypothesis testing. The first one is the type I error, or false positive, in which case the $H_0$ is rejected when there is no effect in reality. On the other hand, the failure to reject the $H_0$ when there is an effect corresponding to the so-called false negative or type II error. In classical statistical methods, there is a pre-specified false positive rate $\alpha$, which, however, is applied on a test-by-test basis and is not suitable for fMRI analysis due to the so-

called multiple testing problem. To illustrate this problem, Poldrack and colleagues (2011) suggest an example in which an image has 100,000 voxels. Given that all voxels with $p < 0.05$ are significant, then 5 % of all voxels, or 5,000 voxels, should be false positives (Poldrack et al., 2011, p. 117). There are two methods that are used to account for the false positive risk over the entire image – the family-wise error rate (FWE or FWER) and the false discovery rate (FDR).

If a threshold of $\alpha_{FWE} = 0.05$ is used, then this means that there is at most a 5% chance of any false positives anywhere in the statistic map. One way of controlling the FWE is the Bonferroni correction, which divides the threshold by the number of tests and therefore controls FWE for any dataset. However, as mentioned earlier, the time courses of voxels are spatially correlated and because of the smoothness of the fMRI data, the Bonferroni procedure is too conservative and may lead to type II error (detecting no signal when there is in fact one). A better way of controlling the FWE is the random field theory (RFT) (Brett, Penny, & Kiebel, 2004; Worsley et al., 1996). RFT depends on assumptions about the distribution of the data and its smoothness, which is measured by FWHM (Full-Width Half-Maximum). FWHM does not only refer to the externally applied smoothing procedure during pre-processing of the data, but also to the intrinsic smoothing mentioned earlier. The smoothness of the data can be considered to be $FWHM_x$ x $FWHM_y$ x $FWHM_z$ (FHWM in each direction) and is expressed in RESELs (resolution of elements in the volume space) (Woolrich, Beckmann, Nichols, & Smith, 2009). The main disadvantage of RFT is that is it still relatively conservative, especially in the case of small group studies. In addition, RFT relies on the assumption that the data is sufficiently smoothed (e.g. with a Gaussian filter whose FWHM is at least twice the voxel dimensions) (Poldrack et al., 2011). An alternative approach for controlling FWE is

using non-parametric methods, such as permutation testing, which uses the distribution of the data itself to find P-values and thresholds (Woolrich, Beckmann, Nichols, & Smith, 2009).

The other approach to the multiple testing problem, FDR, is more relaxed as it controls the proportion of false positives among those that are declared positive. While FWE depends on the number of voxels and the smoothness of data, FDR depends on the amount of signal in the data. Therefore, the larger the signal is, the lower the threshold. Consequently, FDR is more sensitive than FWE for the cost of higher false positive risk. The main disadvantage of FDR is its lack of spatial specificity, i.e. it can provide that, on average, no more than a certain percentage of the voxels present are false positives. (Poldrack et al., 2011).

*3.2.5.7. Cautionary notes*

The multiple-testing problem mentioned above has been very well illustrated by (Bennett, Baird, Miller, & Wolford, 2009a) in their poster focusing on neural correlates in a dead Atlantic salmon and further discussed in (Bennett, Wolford, & Miller, 2009b). Basically, conducting a large number of statistical tests simultaneously will eventually yield some mistakenly ‘significant results’ only by chance. Therefore, as already discussed in the previous section, principled correction methods that provide information on the Type I error rate across the whole brain should be used in the fMRI data analysis (Bennett et al., 2009b).

Principled correction can also be conducted to a predefined region of interest (ROI). In SPM, this can be achieved by using the small-volume correction method, which makes use of Gaussian RFT (Bennett et al., 2009b). However, the ROIs included in the analysis should be predefined and based on a previous, independent dataset. If the ROIs were first defined by a whole-brain exploratory analysis from the

same dataset and then these ROIs were subsequently used for the correlation analysis, this will lead to a non-independent error. This issue was discussed in detail by Vul and colleagues (2009) and caused hot discussions within the scientific community concerning the reliability of fMRI studies in social neuroscience (and in general). The main point is that non-independent analysis methods will lead to results showing unreasonably high correlations, referred to as 'voodoo correlations' by the authors.

### 3.2.6. Connectivity Analysis: Dynamic Causal Modelling

So far, the analysis discussed above delivers information about what brain regions have been activated by a specific task. This activation analysis, often criticised by being called blobology[20], seeks to localise mental function but is unable to offer mechanistic explanations about the connections and interactions between different regions of brain activation. In the past few years, there has been a growing interest in methods dealing with brain connectivity analysis, which can be roughly divided into three categories: anatomical, functional and effective.

Anatomical connectivity focuses on physical connections among different brain regions (e.g. by using diffusion tensor imaging, or DTI). Functional connectivity analysis, on the other hand, deals with undirected associations or correlations in activity between spatially remote brain regions. It seeks to find the predominant pattern of correlations (e.g. by using independent component analysis, or ICA) and has found a widespread use in resting-state fMRI studies. In contrast to functional connectivity, effective connectivity analysis considers the directed influence of one

[20] The term blobology comes from the fact that activated brain regions are illustrated as coloured blobs on human brain maps.

brain area on others, i.e. examines the causal relations among activated brain regions (Friston, 2011).

One of the methods widely used for assessing effective connectivity is Dynamic Causal Modelling (DCM) (Friston, Harrison, & Penny, 2003). DCM is a hypothesis-driven approach for inferring hidden neuronal states from measurements of brain activity (Stephan et al., 2010). It relies on pre-defined biophysical models, built on some prior knowledge about the underlying neuronal network dynamics, and probabilistic (Bayesian) inference methods for accessing the context-specific effects of experimental manipulation. Statistical inference can be of different types: inference on model space, if the interest is focused on aspects of model structure (e.g. serial vs. parallel structure, etc.), and inference on model parameters, if the focus is on the parameters in a model (e.g. excitatory vs. inhibitory connections, etc.) (Stephan et al., 2010).

DCM heavily depends on experimental perturbations and is generally not useful for data analysis when an experimental condition is absent, like in the case of resting-state fMRI (an exception is the newly introduced and currently developed stochastic DCM) (Stephan et al., 2010). Furthermore, prior to the DCM, a conventional SPM analysis needs to be conducted in order to observe if there is any activation in the areas to be studied with DCM. Generally, if no specific activations are detected by the SPM analysis, further analysis using DCM, which is hypothesis-dependent, is not reasonable.

DCM involves a number of different steps. First, the time series for the brain areas of interest need to be extracted from the single-subject data, which will represent the nodes within the DCM. Second, a model space consisting of all potentially plausible models is to be defined. These models can be based, for

instance, on data from previous neuroimaging studies and/or on knowledge about anatomical structures (e.g. by using DTI data or relying on anatomical atlases) and computational processes of the examined neuronal network. A model has the following parameters $\theta = \{A, B, C, h\}$, where $A$ represents the intrinsic connection across the nodes within the model, $B$ stands for the modulatory influence on the nodes by the experimental perturbations, C is the direct influence on the regions in the model, and h is a set of haemodynamic priors. The next step is to estimate the parameters for all DCMs in the model space. Then, the optimal model from the model space needs to be selected by comparing all models. This is typically achieved by using Bayesian model selection (BMS), which chooses the model with best balance between accuracy and complexity. Increase in model complexity leads to increased model fit but decreased generalizability. Too complex models should be avoided as they may result into 'over-fitting': fitting noise that is specific to a data set (Stephan et al., 2007). Finally, statistical tests are conducted on the parameters of the optimal model to test the hypothesis in question.

An alternative approach to BMS is Bayesian model averaging (BMA), especially in cases when none of the models significantly outperforms all other ones or when parameter estimates across different groups (e.g. patients and healthy controls) need to be compared. BMA makes use of the whole model space and computes averages of each model parameter weighted by the posterior probability for each model (Stephan et al., 2010).

Although DCM can deliver interesting results about the causal connectivity within a certain neuronal network, it faces some shortcomings and challenges (for a more detailed discussion, refer to Lohmann, Erfurth, Müller, & Turner, 2012 and Daunizeau, David, & Stephan, 2011). For instance, it heavily depends on the model

space and can therefore deliver misleading results in case the pre-defined models are not plausible, since DCM cannot recognise the implausible models or the ones that do not explain the data (Lohmann, Erfurth, Müller, & Turner, 2012). DCM is also criticised for its inability to be adequately applied to more complex network structures in which the increasing number of regions and inputs leads to combinatorial explosion. Still, while its reliability for exploratory applications is still a matter of discussion, its use for biologically plausible models within the scope of cognitive neurosciences is proving very promising.

## *3.3. Summary*

This chapter aimed at introducing the basic principles of the neuroimaging method of fMRI, used for the empirical study discussed below. In order to understand the methodological aspects of the study, topics concerning the basic physics of MRI, the nature of the BOLD fMRI signal, fMRI study design, and data analysis have been discussed in some details in this part of the thesis. The following chapter deals with an empirical fMRI study conducted with SAD patients and healthy control participants and focuses on the neurobiological models and hypotheses discussed at the beginning of the thesis.

# IV. fMRI Study

## *4.1. Background*

As discussed earlier, social anxiety disorder (SAD) is a psychiatric condition in which people suffer from intense dread of social situations and of other people's scrutiny. Since its recognition as a disease by the APA in the 1980s, there has been a growing interest in the research of SAD.

Studies focusing on its neural correlates have confirmed the central role of the limbic system and the amygdala in particular (Davis & Whalen, 2001; Phelps & LeDoux, 2005), with the amygdala being hyperactive in SAD patients, relative to healthy controls (HCs), during the perception of emotional facial expressions (Ball et al., 2012; Klumpp, Angstadt, & Phan, 2012; Phan et al., 2006; Stein, 2002). Other studies have observed similar results using different types of stimuli that can be considered to be anxiety-inducing for SAD patients, such as reading negative comments referring to themselves (Blair et al., 2011), perception of social situations illustrated in images (Nakao et al., 2011), speech anticipation (Tillfors et al., 2001), direct eye gaze (Schneier, Kent, Star, & Hirsch, 2009; Schneier, Pomplun, Sy, & Hirsch, 2011), and situations involving uncertainty (Krain et al., 2008).

In addition to the amygdala, it has also been suggested that the default-mode network (DMN), which is active in resting state or during task-independent introspection and self-referential thought, shows some sub-normalities in SAD patients and in particular decreased functional connectivity between the frontal and occipital areas (Ding et al., 2011). Furthermore, SAD-specific altered activations have been observed in regions within the prefrontal cortex, implicated in the voluntary emotion regulation (Brühl et al., 2011; Labuschagne et al., 2011; Monk et al., 2008;

Phillips et al., 2008; Tröstl et al., 2011; Sladky et al., 2012). The functional connectivity within the amygdalar-prefrontal network has also been confirmed by various resting-state fMRI studies (Ding et al., 2011; Hahn et al., 2011; Liao et al., 2010; Qiu et al., 2011). Specifically, the dorsolateral prefrontal cortex (DLPFC), which is believed to be implicated in selecting, implementing, and monitoring of cognitive control and executive strategies for regulation of (negative) emotional affects (Ochsner & Gross, 2005), has shown greater activation in SAD patients relative to HCs (Brühl et al., 2011), which can be explained by the presence of increased self-focused thoughts typical in SAD. With regard to the orbitofrontal cortex (OFC), which is also implicated in the down-regulations of emotions, the results from different studies are inconclusive: ranging from decreased activity in SAD patients as compared to healthy participants (Hahn et al., 2011; Tillfors et al., 2001) to no significant difference between the two groups (Nakao et al., 2011; Schneier et al., 2009).

While the disruption of the amygdalar-prefrontal circuitry typical of SAD has been generally confirmed, the exact mechanisms behind the network, including the regions of amygdala, OFC and DLPFC, is still not well-understood and is a subject of further research (e.g. Sladky et al., 2012). Additionally, the question about the effect that attention has on emotional processing is still open. Various studies have dealt with this issue, some giving support for bottom-up processing of (emotional) stimuli of evolutionary significance like fear of threat (Schupp et al., 2003), independent of task-relevant attentional operations (Fenker et al., 2010), while others emphasising on the impact of attentional load and the available perceptual resources on the emotional processing (Blair et al., 2007; Pessoa et al., 2005; Schultz & Heimberg, 2008; Silvert et al., 2007).

The aim of the current fMRI study is to provide further evidence for the role of the amygdalar-prefrontal network in SAD patients. For this purpose, the emotional Stroop task proposed by Blair and colleagues (2007) will be used, in which emotional faces serve as distractors during a goal-directed processing task. Our main focus is on the interplay between emotion and cognition in the clinical context of SAD. More specifically, our first hypothesis deals with the impact of goal-directed processing, and attentional load in particular, on the processing of emotional distractors and will address the following question:

1. Is amygdala hyperactive in SAD patients relative to healthy participants during the perception of harsh faces, irrespective of the attentional load of the cognitive task?

The second hypothesis we would like to address deals with the impact of the emotional distractors on the goal-directed processing and seeks to answer the following question:

2. Does the presence of emotional distractors lead to the recruitment of pre-frontal regions aiming at amygdalar down-regulation?

We expect to observe increased amygdalar activation in SAD patients when exposed to negative emotional faces irrespective of the task and increased pre-frontal activation, especially during higher attentional load, serving as a down-regulatory mechanism for the amygdalar hyper-activation.

## *4.2. Methods and Materials*

### 4.2.1. Participants

15 patients with social anxiety disorder (7 males and 8 females, mean age ± SD: 26.6 ± 8.6 years) and 15 matched healthy control (HC) participants (8 males and 7 females, mean age ± SD: 25.4 ± 3.4 years) took part in the study. All participants provided written informed consent prior to the study and were financially reimbursed for their participation. The study protocol was approved by the Ethics Committee of the Medical University of Vienna.

Both SAD patients and HCs underwent a clinical assessment administered by the clinical personnel of the Department of Psychiatry of the General Hospital in Vienna. None of the participants had any history of neurological or psychiatric disorders, with the exception of SAD in the patient group. Additional exclusion criteria included pregnancy, current or prior history of substance abuse, or any psychotropic medication within the last three months. On the day of the experiment, a compulsory drug screening was conducted using ToxiQUICK PAN-10 test panels (ACON Laboratories, San Diego, USA).

To be included in the study, the SAD patients were diagnosed using the German version of the Structured Clinical Interview for DSM-IV (SCID) (First, Spitzer, Gibbon, & Williams, 1996). Additionally, all participants completed the State-Trait Anxiety Inventory, State (STAI-S) and Trait (STAI-T) versions (Spielberger, Gorssuch, Lushene, Vagg, & Jacobs, 1983), as well as Hamilton Anxiety Rating Scale (HAM-A) (1959), and Liebowitz Social Anxiety Scale (LSAS) (Liebowitz, 1987). Based on the psychometric scores, the SAD patients reported greater levels of social

anxiety on the LSAS and HAM-A, and state and trait anxiety on the STAI. The results from the psychometric assessment are shown in Figure 3:

| | Age | HAM-A | STAI (state) | STAI (trait) | LSAS |
|---|---|---|---|---|---|
| SAD | $26.6 \pm 8.6$ | $16.9 \pm 5.0$ | $42.1 \pm 12.8$ | $52.2 \pm 11.2$ | $75.6 \pm 22.7$ |
| HC | $25.4 \pm 3.4$ | $0.5 \pm 0.6$ | $25.6 \pm 3.3$ | $27.0 \pm 4.8$ | $5.3 \pm 7.3$ |
| p (two-tailed) | $> 0.6$ | $< 0.001$ | $< 0.001$ | $< 0.001$ | $< 0.001$ |

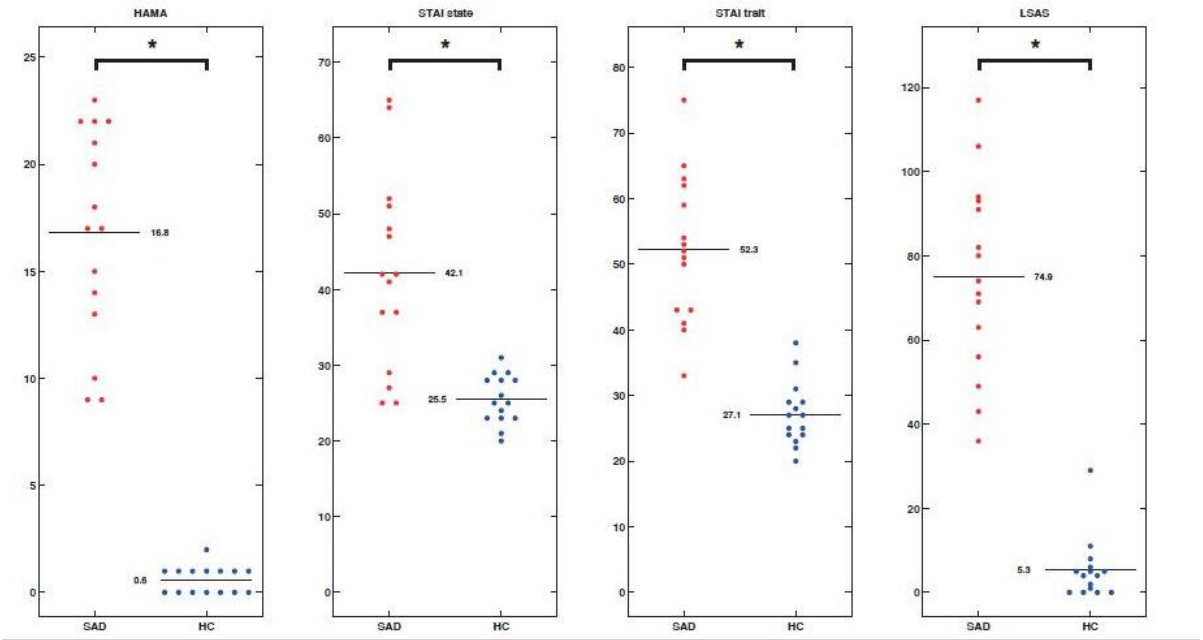


Figure 3. Psychometric assessment of participants *(mean scores ± SD for SAD patients and healthy control group): Hamilton Anxiety Rating Scale (HAM-A), Spielberger State-Trait Anxiety Inventory for Adults (STAI), and Liebowitz Social Anxiety Scale (LSAS)* [21]

### 4.2.2. Task

The Affective Stroop task of Blair et al. (2007) (Blair et al., 2007) was adapted for the current study. In this task, participants were presented sequentially with two numerical displays in the form of a 3 x 3 matrix consisting of numbers and asterisks. Between the presentations of the numerical displays, a distractor in the form of a neutral or a harsh face was shown. Forty neutral and forty harsh faces designed

[21] Source: Sladky et al. (2012)

using the NimStim Set of Facial Expressions (MacArthur Foundation Research Network on Early Experience and Brain Development; http://www.macbrain.org/resources.htm) were included in the study. An example of the presentation stimuli can be seen in Figure 4. The participants had to decide which display contained the greater numerosity (e.g. 4 greater than 2, irrespective of the number of digits presented). The task fulfilled three different conditions: congruent (the number of digits corresponded to the numerosity), incongruent (the number of digits differed from the numerosity), and fixation condition, in which no numerical display was shown. The conditions were presented in a randomised order and a crosshair, with jittered presentation duration (800 ms ± 200 ms), was shown briefly between the task events.

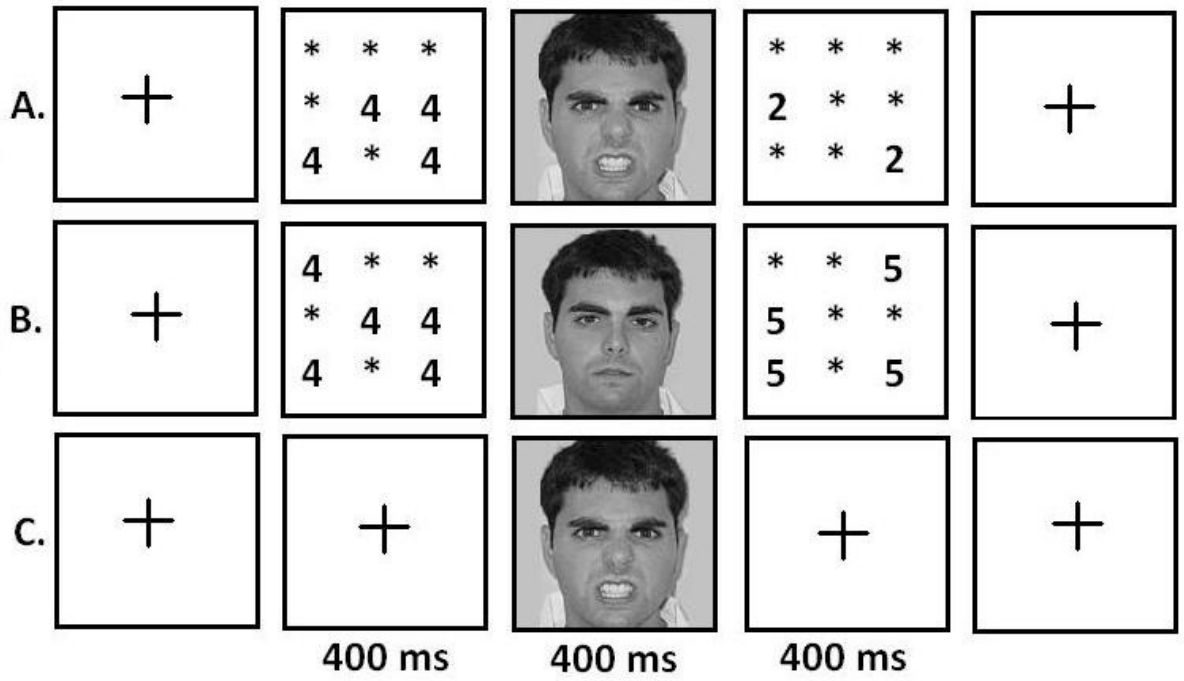


Figure 4. fMRI study stimuli
*Example of trial sequences: A. Congruent harsh trial (CH), B. Incongruent neutral (IN); C. Fixation harsh trial (FH)*

### 4.2.3. Image acquisition

Participants were scanned in a 3 Tesla TIM TRIO MR Scanner (Siemens Medical, Erlangen, Germany) using the manufacturer's 32-channel head coil. 225 whole-brain volumes with a matrix size of 128 x 128 $px^2$ x 20 slices were acquired at a repetition time of TR = 1.8 s using a single-shot echo planar imaging (EPI) sequence (TE = 40 ms, FOV = 190 x 190 $mm^2$, voxel size = 1.48 x 1.48 x 3 $mm^3$, slice thickness = 3 mm, inter-slice gap = 2.1 mm, and bandwidth = 1446 Hz/px). The purpose of the relatively high spatial resolution was to minimise MRI signal losses in the ventral brain regions due to the local field inhomogeneities leading to intra-voxel dephasing effects (Robinson, Windischberger, Rauscher, & Moser, 2004).

### 4.2.4. Preprocessing and data analysis

Data preprocessing and the statistical analysis were conducted in SPM8 (FIL Group, UC London, UK). The preprocessing pipeline included slice timing correction (Sladky et al., 2011), compensating for the time shift in acquisition, motion correction (or realignment) in order to exclude artefacts due to bulk head movement, segmentation, normalisation to standard MNI space (at 2 mm isotropic voxel size), and spatial smoothing using an isotropic Gaussian kernel of 8 mm FWHM in order to reduce inter-subject variability and allow for a group analysis.

For the first-level (within-subject) analysis, the General Linear Model (GLM) implemented in the SPM8 software was used. Regressors for each of the response types (i.e. 6 regressors for the 6 conditions) were created by convolving the stick functions of the onsets with the SPM8's canonical haemodynamic response function (HRF). Additionally, all six realignment parameters, resulting from the pre-processing

motion correction step, were included into the design matrix as regressors of non-interest in order to compensate for residual motion effects. The following contrasts were created: effects of interest (an F contrast across all six regressors of interest), T contrasts for valence (i.e. harsh > neutral and neutral > harsh), and T contrasts for task (i.e. congruent > incongruent, incongruent > congruent, task > fixation, and fixation > task). The first-level analysis created a beta coefficient and its associated t-statistic for each voxel and each regressor.

Second-level (group) analysis was conducted with whole-brain ANOVAs using the beta images from the first-level analysis. First, the main effects of the experimental design were tested using a full factorial ANOVA design with the following two factors: valence (including 2 levels: harsh and neutral) and task (including 3 levels: congruence, incongruence and fixation) across both groups. In addition, two separate flexible factorial ANOVA designs, for the two groups respectively, were performed in order to produce group-specific statistical parametric maps of the main effect of emotion, task and interaction of emotion and task. Both ANOVAs involved a 2 (valence: harsh, neutral) by 3 (task: congruent, incongruent, fixation) design and examined the interactions of emotion and task. Furthermore, a three-way factorial design with two within-subject factors (Valence: neutral and harsh; Task: congruence, incongruence, and fixation) and one between-subject factor (Group: HC and SAD) was used to test for differences between the two groups with respect to emotion and task. For comparison purposes, the same three-way factorial analysis was repeated in GLM Flex by Aaron Schultz (available at http://nmr.mgh.harvard.edu/harvardagingbrain/People/AaronSchultz/GLM_Flex.html). Also, four two-sample t-tests were conducted for the following contrasts: harsh>neutral, incongruent>congruent, task>fixation, fixation>task.

Finally, a follow-up analysis on the nature of the interactions was conducted. Spherical regions of interest (ROIs) were defined around the peak voxels revealed in the second-level analysis using the contrast for activation differences between harsh versus neutral stimuli. Percent signal change was calculated for the ROIs for each participant separately using Marsbar (Brett et al., 2002). For the main effect of emotion, a paired t-test was used to compare the percent signal change of negative vs. neutral trials collapsed across task (congruent, incongruent, fixation), separately for each group. Similarly, for the main effect of task, the percent signal change of congruent, incongruent and fixation trials, collapsed across valence (negative, neutral) was compared. Two-sample t-tests were used to compare the percent signal change between the two groups.

## *4.3. Results*

### 4.3.1. Behavioural data

Reaction times (RTs) and accuracy in performance were compared between the two experimental groups, using the IBM SPSS Statistics software, Version 20.0 (2011). Mean RTs were computed for each participant (see Table 1 below) and the effects of emotion and task on RTs were examined using a 2 (emotion: negative, neutral) by 2 (task: congruent, incongruent) repeated measures ANOVA. There was neither a significant main effect of task ($F(1,29) = 7.23$, $p < 0.012$), nor a significant main effect of emotion ($F(1,29) = 0.00$, $p < 1.00$).

| Valence | Task | Group | RTs (±SD) in ms | Accuracy (in %) |
|---|---|---|---|---|
| Neutral | Congruent | HC | 756 (± 249) | 95 (± 4) |
| | | SAD | 834 (± 290) | 97 (± 2) |
| | Incongruent | HC | 818 (± 332) | 94 (± 7) |
| | | SAD | 844 (± 270) | 96 (± 3) |
| Harsh | Congruent | HC | 730 (± 217) | 94 (± 6) |
| | | SAD | 816 (± 328) | 96 (± 4) |
| | Incongruent | HC | 745 (± 227) | 94 (± 7) |
| | | SAD | 829 (± 297) | 98 (± 4) |

Table 1. Behavioural analysis. *RTs and accuracies across groups and conditions*

### 4.3.2. fMRI data

#### *4.3.2.1. Task-related effects*

Similarly to the approach used for the behavioural data, the first part of the fMRI analysis involved a 2 (emotion: negative, neutral) by 3 (task: congruent, incongruent, fixation) ANOVA examining the effects of task and emotion involving negative vs. neutral stimuli for both groups. The results are summarised in Table 2 below.

Regions showing a differential BOLD response to negative stimuli included: bilateral amygdala, right fusiform gyrus, orbitofrontal cortex (OFC), bilateral inferior and dorsolateral prefrontal cortex (DLPFC), left superior frontal gyrus, left supplementary motor area (SMA), and left inferior temporal gyrus. BOLD signal changes related to the cognitive task condition irrespective of attentional load were observed in the left precentral gyrus, right supramarginal gyrus, right insula, right cerebellum, and frontal regions including bilateral middle frontal gyrus and right superior frontal gyrus.

| Regions | Coord. MNI [mm] | | | Peak level | | | |
|---|---|---|---|---|---|---|---|
| Anatomy | x | y | z | $D_{FWE\text{-}corr}$ | $q_{FDR\text{-}corr}$ | T | Z |
| harsh > neutral* | | | | | | | |
| R fusiform gyrus | 40 | -52 | -18 | 0.006 | 0.022 | 5.35 | 5.13 |
| OFC, orbitofrontal cortex | 4 | 50 | -16 | 0.011 | 0.022 | 5.19 | 4.98 |
| R amygdala | 20 | -8 | -14 | 0.962 | 0.757 | 3.52 | 3.45 |
| L amygdala | -18 | -10 | -14 | 0.089 | 0.080 | 4.63 | 4.48 |
| L inferior and DLPFC | -40 | 36 | -12 | 0.152 | 0.092 | 4.47 | 4.34 |
| R inferior and DLPFC | 58 | 34 | 16 | 0.999 | 0.861 | 3.24 | 3.19 |
| L superior frontal gyrus | -10 | 54 | 34 | 0.097 | 0.080 | 4.61 | 4.46 |
| L supplementary motor area | -8 | 10 | 62 | 0.125 | 0.088 | 4.53 | 4.39 |
| L inferior temporal gyrus | -40 | -30 | -18 | 0.189 | 0.092 | 4.40 | 4.27 |
| neutral > harsh | | | | | | | |
| R precuneus | 14 | -66 | 48 | 0.000 | 0.002 | 6.80 | 6.37 |
| L insula | -42 | -2 | 10 | 0.001 | 0.117 | 5.74 | 5.47 |
| incongruent > congruent | | | | | | | |
| R inferior occipital gyrus | 46 | -80 | -2 | 0.000 | 0.000 | 9.90 | >4.0 |
| L supplementary motor area | -2 | -4 | 56 | 0.000 | 0.000 | 9.46 | >4.0 |
| R middle frontal gyrus | 34 | -4 | 58 | 0.000 | 0.000 | 8.52 | 7.73 |
| L insula | -24 | 4 | 2 | 0.000 | 0.000 | 8.13 | 7.43 |
| L thalamus | -10 | -20 | 6 | 0.000 | 0.000 | 7.60 | 7.01 |
| R insula | 34 | 22 | 4 | 0.000 | 0.000 | 7.23 | 6.72 |
| R superior temporal gyrus | 52 | -42 | 14 | 0.000 | 0.000 | 6.74 | 6.32 |
| R thalamus | 8 | -18 | 4 | 0.000 | 0.001 | 6.54 | 6.15 |
| congruent > incongruent* | | | | | | | |
| L precuneus | -8 | -54 | 12 | 0.069 | 0.249 | 4.70 | 4.55 |
| L superior frontal gyrus | -14 | 56 | 18 | 0.166 | 0.249 | 4.45 | 4.31 |
| L interior frontal gyrus | -26 | 30 | -16 | 0.333 | 0.259 | 4.21 | 4.10 |
| L middle frontal gyrus | -18 | 26 | 40 | 0.462 | 0.283 | 4.08 | 3.97 |
| OFC, orbitofrontal cortex | -2 | 34 | 10 | 0.685 | 0.422 | 3.88 | 3.79 |
| task > fixation | | | | | | | |
| L precentral gyrus | -38 | -22 | 62 | 0.000 | 0.000 | 16.68 | >4.0 |
| R supramarginal gyrus | 46 | -24 | 36 | 0.000 | 0.000 | 8.82 | >4.0 |
| R insula | 42 | 0 | 16 | 0.000 | 0.000 | 7.99 | 7.32 |
| R cerebellum | 14 | -50 | -20 | 0.000 | 0.000 | 12.39 | >4.0 |
| L middle frontal gyrus | -36 | 40 | 30 | 0.000 | 0.002 | 6.31 | 5.95 |
| R middle frontal gyrus | 40 | 42 | 24 | 0.000 | 0.000 | 6.95 | 6.49 |
| R superior frontal gyrus | 26 | 0 | 58 | 0.000 | 0.001 | 6.51 | 6.12 |
| fixation > task | | | | | | | |
| L middle occipital gyrus | -34 | -88 | -4 | 0.000 | 0.000 | 7.48 | 6.92 |
| R fusiform gyrus | 36 | -44 | -16 | 0.000 | 0.003 | 6.61 | 6.21 |
| L fusiform gyrus | -28 | -44 | -14 | 0.001 | 0.037 | 5.88 | 5.59 |
| OFC, orbitofrontal cortex | 2 | 48 | -16 | 0.002 | 0.098 | 5.58 | 5.33 |
| R amygdala* | 22 | -10 | -18 | 0.498 | 0.143 | 4.05 | 3.94 |

Table 2. Task-related effects. *All activations are observed in whole brain analyses significant at p<0.05 FWE corrected, n= 75 voxel minimum cluster size, except * significant at p<0.001 uncorrected for multiple comparisons.*

Higher attentional load (i.e. during the incongruent condition) led to greater activation in right inferior occipital gyrus, left SMA, right middle frontal gyrus, right superior temporal gyrus, bilateral insula, and bilateral thalamus. During the fixation condition, greater activation was observed in the left middle occipital gyrus, bilateral fusiform gyrus, OFC, and right amygdala. No interaction between task and valence was observed at p<0.001 uncorrected for multiple comparisons.

*4.3.2.2. Group-related effects*

The results from the two separate flexible factorial designs are illustrated in Figure 5 below.

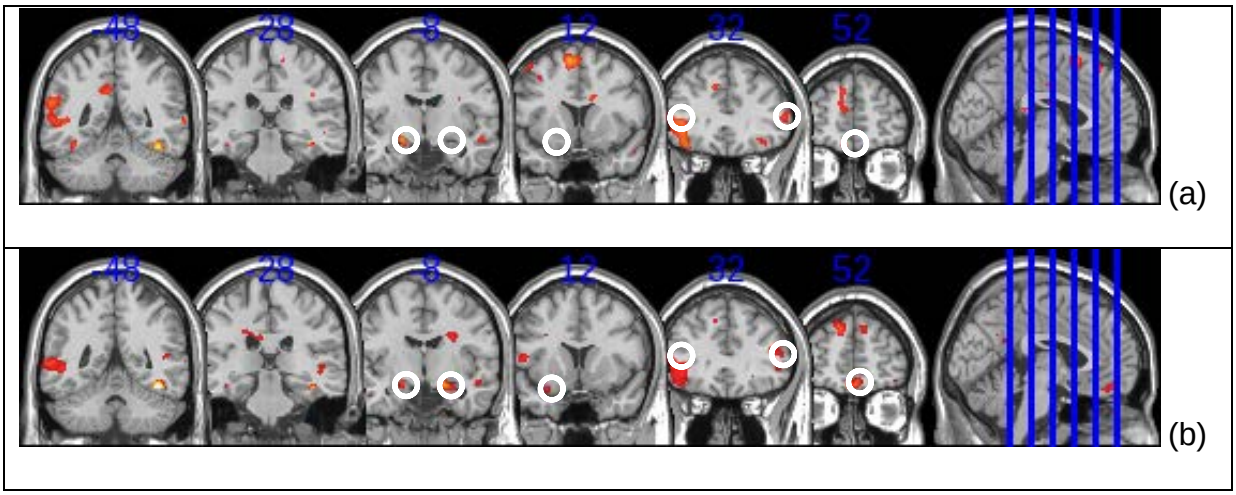


Figure 5. SPMs from second-level flexible factorial analyses. *HC (a) and SAD (b); contrast of interest: harsh vs. neutral (p<0.05 uncorrected, n = 75 voxels minimum cluster size, $T_{max}$ = 7.02). ROIs, including bilateral amygdala, bilateral DLPFC and OFC, are marked with white circles.*

While a similar pattern of activation can be observed in both groups, there is a greater OFC activation in the SAD relative to the HC group, while the right amygdala is activated in the SAD group only. However, these results should be considered with caution, since the activations were only significant at p<0.05 uncorrected for multiple comparisons and did not survive any FWE or FDR correction on both peak and cluster levels.

The three-way full factorial design, including the factors group, valence and task, was used to test for the interactions of group with valence or task and did not show any significant activations in the regions of interest discussed in the previous section. The interaction between group and task showed BOLD increase only in the left precentral gyrus (x,y,z = -37, -32, 57; F=12.31, $p_{FWE\text{-}corr}$=0.227) and the SMA (x,y,z = -4, -4, 60; F=16.11, $p_{FWE\text{-}corr}$=0.015), while the interaction between group and valence did not yield any significant results at p<0.001 uncorrected for multiple comparisons. The same results were observed using the GLM Flex. The additional analysis using the two-sample t-tests also did not identify any significant group differences at p<0.001 uncorrected for multiple comparisons.

*4.3.2.3. ROI analysis*

The subsequent analysis included the following ROIs: bilateral amygdala, bilateral DLPFC, and OFC, which were identified within the second-level analysis testing for task-related effects (see Table 2: harsh>neutral, as well as Figure 5 above). Not all ROIs were activated in the SPMs from the first-level analysis and, consequently, only those participants who showed activation were included in the ROI analysis (i.e. OFC: 11 HC, 13 SAD; left amygdala: 11 HC, 8 SAD; right amygdala: 8 HC, 9 SAD; left DLPFC: 11 HC, 12 SAD; right DLPFC: 11 HC, 11 SAD). Results are illustrated in Figure 6 below.

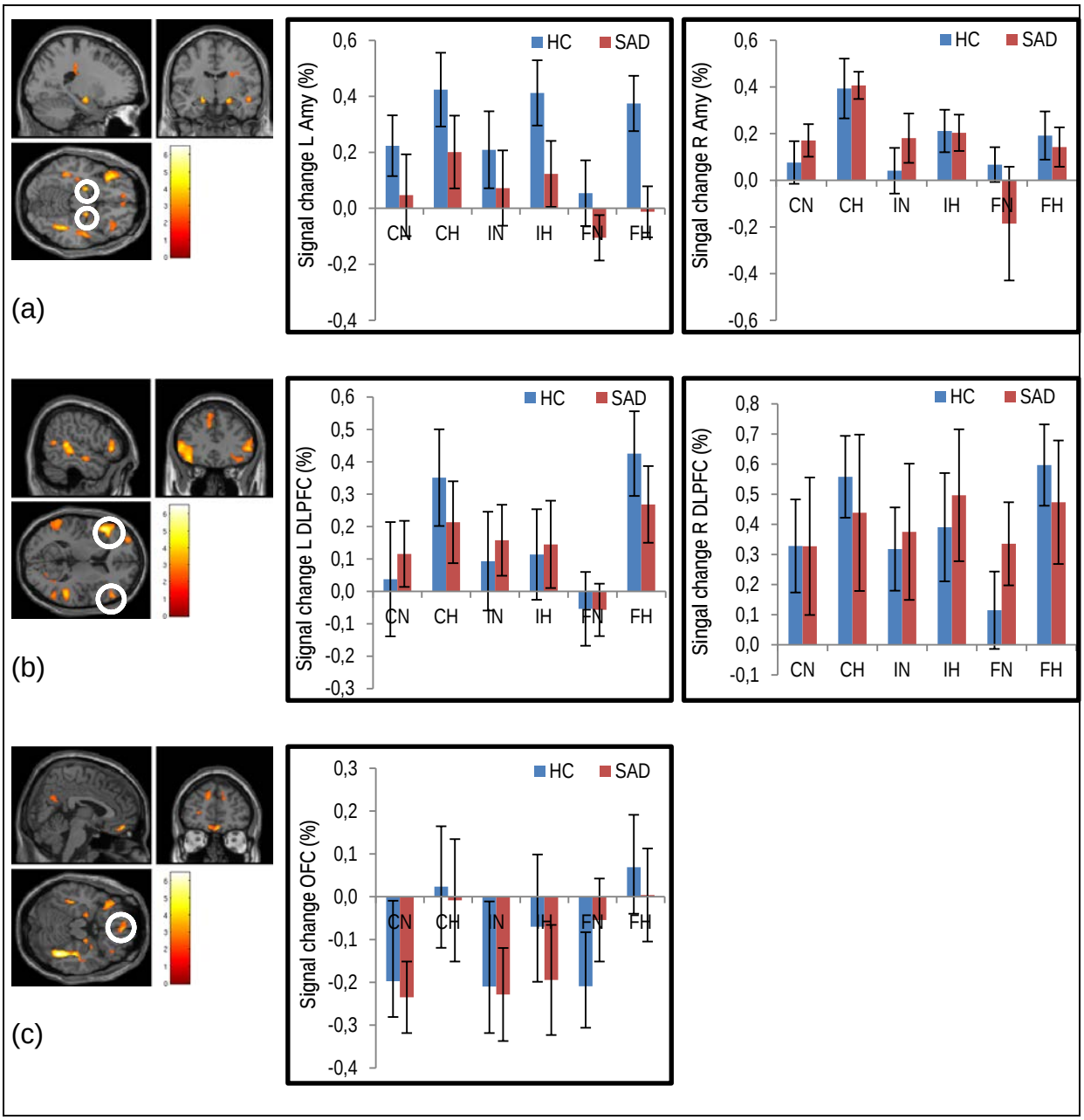


Figure 6. Response to task involving negative stimuli. *(a) left (x,y,z=-18,-10,-14) and right (x,y,z=20,-8,-14) amygdala, (b) left (x,y,z,=-40,36,-12) and right (x,y,z=58,34,-12) DLPFC, (c) OFC (x,y,z=4,50,-16). Bar errors represent SEM. Abbreviations: CN = congruent neutral, CH = congruent harsh, IN = incongruent neutral, IH = incongruent harsh, FN = fixation neutral, FH = fixation harsh (SPMs at p>0.02 uncorr.)*

The left amygdala was more strongly activated in the HC group relative to the SAD group. In both groups, activation was greater during harsh stimuli. Similar trend is present for the right amygdala but with slightly stronger BOLD response in SAD relative to HC. It is surprising to note that in SAD patients the BOLD signal decreases

during the incongruent condition relative to the congruent one. Higher cognitive load (i.e. incongruent condition) also results in slightly higher DLPFC activation in SAD patients, as opposed to lower cognitive load (i.e. congruent condition). The OFC was more strongly activated during the fixation condition as opposed to the task condition.

## *4.4. Discussion*

In this study, we used an emotional Stroop task paradigm to investigate the interplay between emotion and cognition in SAD patients as compared to healthy controls. We expected to find further evidence for the role of the amygdalar-prefrontal network in emotion perception in SAD patients. The main focus was on the following regions of interest: the bilateral amygdala, the medial orbitofrontal cortex, and the bilateral dorsolateral prefrontal cortex, which are reported to be involved in the anxiety-regulating network in SAD (Phillips et al., 2008; Tröstl et al., 2011; Sladky et al., 2012). The task-related effects showed that all the regions of interest were activated during the perception of negative stimuli, which suggests the sensitivity of the chosen task for investigating the limbic-cortical network, involved in emotional processing.

### *4.4.1. Amygdala activation*

Our first hypothesis sought to answer the question whether the amygdala is hyperactive in SAD patients relative to HC during the perception of harsh faces and what impact the attentional load has on the emotional processing. The results suggested that there were no significant group differences. It is interesting that the separate flexible factorial analyses showed an increased activation of left amygdala in HC, while the SAD group has an increased BOLD response of the right amygdala (Figure 5). The same trend but lateralised activity was also evident from the ROI analysis (Figure 6a). While a significant body of research has consistently reported

amygdala activation during emotion processing, it is inconclusive whether there is a clear-cut hemisphere-specific difference between the right and left amygdala (see Baas, Aleman, & Kahn, 2004 for a systematic review of previous studies).

One of the proposed hypotheses is that the right amygdala is engaged in fast analysis of emotional stimuli, while the left amygdala is involved in more detailed feature extraction (Markowitsch, 1998; Phelps et al., 2001). A similar hypothesis is proposed by Glascher and Adophs (2003) suggesting that the right amygdala is first automatically activated by emotional stimuli, while the left amygdala is engaged in cognitive perceptual emotional information processing (cited in Baas et al. 2004, p. 97). Wright and colleagues (2001), who support this hypothesis of laterality of amygdalar activation, also suggest that the right amygdala habituates faster than the left one. In the light of this framework and our findings, it can be argued that SAD patients processed the negative stimuli in a bottom-up fashion, irrespective of the cognitive task. Habituation effects have not been tested in the present study; however, previous research (Sladky et al. 2012) showed habituation differences in bilateral amygdala between SAD patients and HC but did not provide any evidence for a differential habituation between the two hemispheres, as proposed by Wright et al. (2001). However, it is important to note that Sladky and colleagues (2012) observed gradual habituation of the emotional processing network in SAD following increasing experience with the emotion discrimination task used in the experiment. Since the present emotional Stroop task was conducted shortly after the above-mentioned emotion discrimination task and both experiments include similar stimuli (i.e. emotional faces), the lack of significant amygdalar hyperactivation in SAD in our experiment could possibly be explained by carry-over habituation effects from the previous experiment.

All in all, the amygdala was activated by the presence of the harsh faces, as expected, and it seems that the cognitive task did not interfere with the perception of the emotional stimuli, as we did not observe differential activation between the task and fixation condition. If the attentional load interfered with the emotional processing, then we must have been able to notice a decrease of amygdala activation during the task and especially during the incongruent condition and increased activation during the fixation condition, when there was no cognitive task but only faces were displayed. The lack of strong indication for amygdalar hyperactivity in SAD patients relative to HC might also be due to the small sample size used for the study, which can lead to reduced statistical power and sensitivity. During manual inspection of the individual data, we observed some heterogeneity of activation patterns in SAD patients. Such within-group differences are not surprising, as psychiatric diseases can have varying symptoms and causes, but should be compensated for by including a bigger sample size for instance.

An alternative explanation for the lack of amygdalar hyperactivation could be that the scanning situation itself was too anxiety-inducing and the SAD patients felt anxious not only when exposed to the harsh facial stimuli, but also during the whole scanning session. Since fMRI is an indirect method measuring differences in BOLD signal, the existence of a baseline (i.e. when a participant is not anxious) is essential.

*4.4.2. Prefrontal activation*

With regard to our second hypothesis, we expected that the emotional stimuli will have such an impact on the cognitive task in SAD patients that the need to down-regulate the amygdalar activation will lead to an increased prefrontal activation during the task condition. This expectation was not met in the case of the orbitofrontal cortex, which was slightly more active in the HC group relative to the SAD group

during the fixation task and to a lesser extent during the congruent condition but not during the incongruent one (Table 2, Figure 6c).

In the case of the bilateral DLPFC, there is a trend showing a slight increase in the BOLD signal in SAD patients relative to HC during the incongruent condition, but not during the congruent or fixation conditions, which provides some support for the down-regulating function of the DLPFC within the limbic-cortical circuit. Furthermore, the DLPFC was active only during the harsh>neutral contrast but not vice versa, which suggests a differential activation during emotional processing. It should be noted, however, that these activations were viewed at a low threshold and have not been corrected for multiple comparisons and should therefore be considered with caution.

## *4.5. Conclusion*

To summarise, we could identify a regulatory limbic-cortical neuronal circuit involving the amygdala and prefrontal regions, and more specifically the orbitofrontal cortex and dorsolateral prefrontal cortex. However, we did not succeed in clearly identifying between-group differences, which might be due to habituation effects or weak specificity of the experimental task. However, despite the inconclusive results, there is no clear evidence for an alternative hypothesis of emotional processing in SAD patients. In order to further analyse our hypotheses, it may be necessary to increase the sample size used for the study and conduct further follow-up analyses. For instance, it would be of main interest to investigate the causal relationships within the identified brain network, which is currently being conducted in the research group. For this purposes, the dynamic causal modelling approach, discussed earlier in this thesis, can be applied. However, as already mentioned, this is hypothesis-driven

approach which can be applied only if all the ROIs in a network are activated on individual level. Furthermore, multimodal analyses, if available, including resting state fMRI and diffusion tensor imaging (DTI) data, can provide a good opportunity for a more elaborate assessment of the brain network involved in emotional processing in SAD patients by combining structural and functional imaging information together. Finally, to ensure the generalizability of the results, it would be of interest to investigate whether the findings also apply to the previously discussed subtype of SAD patients, deviating from the stereotypical shy and submissive persons (Kashdan & McKnight, 2010), as it might be possible that such a subgroup exhibit slightly different neuronal activation patterns.

# V. Summary

Anxiety in itself can be very useful, as it alters our behaviour in advantageous ways during a threatening situation. However, when fear becomes maladaptive, it can have severe effects on everyday life and its quality, as well as for the person's health and well-being.

The topic of the current thesis was Social anxiety disorder (SAD), which is a complex psychiatric condition, affecting a large number of individuals around the world. The theoretical part of the thesis dealt with some historical underpinnings, formal theories and models of emotional processing and cognition, as well as with the physics and the methodological aspects of functional magnetic resonance imaging, which were then used as a basis for the experimental part of the thesis.

Within the experimental study, we investigated the brain network of SAD by focusing on the interplay between emotion and cognition. For this purpose, we used a previously applied study design involving an emotional Stroop task. We provided further evidence for the involvement of a limbic-cortical network in the processing of emotional stimuli but failed to identify group differences between patients and controls. At the end of the experimental chapter, ideas for improvements and further research were mentioned, which can facilitate a better understanding of the neuronal circuitry of the disorder and provide evidence for valid neurobiological models, essential for further advancements in therapeutic research.

# VI. Bibliography

Acarturk, C., Cuijpers, P., van Straten, A., & Graaf, R. de. (2009). Psychological treatment of social anxiety disorder: a meta-analysis. *Psychological medicine*, *39*(2), 241–254. doi:10.1017/S0033291708003590

Adolphs, R., & Damasio, A. R. (2000). Neurobiology of emotion at a systems level. In J. C. Borod (Ed.), *The neuropsychology of emotion* (pp. 194–213). New York: Oxford University Press.

Arthurs, O. J., & Boniface, S. (2002). How well do we understand the neural origins of the fMRI BOLD signal? *Trends in Neurosciences*, *25*(1), 27–31. doi:10.1016/S0166-2236(00)01995-0

Baas, D., Aleman, A., & Kahn, R. (2004). Lateralization of amygdala activation: a systematic review of functional neuroimaging studies. *Brain Research Reviews*, *45*, 96–103. doi:10.1016/j.brainresrev.2004.02.004

Ball, T. M., Sullivan, S., Flagan, T., Hitchcock, C. A., Simmons, A., Paulus, M. P., & Stein, M. B. (2012). Selective effects of social anxiety, anxiety sensitivity, and negative affectivity on the neural bases of emotional face processing. *NeuroImage*, *59*(2), 1879–1887. doi:10.1016/j.neuroimage.2011.08.074

Beck, A. T., & Clark, D. A. (1997). An information processing model of anxiety: automatic and strategic processes. *Behaviour research and therapy*, *35*(1), 49–58.

Beck, A. T., Emery, G., & Greenberg, R. L. (1985). *Anxiety disorders and phobias: A cognitive perspective* (15th ed.). Cambridge, MA: Basic Books.

Bennett, C. M., Miller, M. B., & Wolford, G. L. (2009a). Neural correlates of interspecies perspective taking in the post-mortem Atlantic Salmon: an argument for multiple comparisons correction. *Organization for Human Brain Mapping 2009 Annual Meeting*, *47, Supplement 1*(0), S125. doi:10.1016/S1053-8119(09)71202-9

Bennett, C. M., Wolford, G. L., & Miller, M. B. (2009b). The principled control of false positives in neuroimaging. *Social Cognitive and Affective Neuroscience*, *4*(4), 417–422. doi:10.1093/scan/nsp053

Blair, K. S., Geraci, M., Otero, M., Majestic, C., Odenheimer, S., Jacobs, M., Blair R.J & Pine, D.S. (2011). Atypical modulation of medial prefrontal cortex to self-referential comments in generalized social phobia. *Psychiatry Research: Neuroimaging*, *193*(1), 38–45. doi:10.1016/j.pscychresns.2010.12.016

Blair, K., Smith, B., Mitchell, D., Morton, J., Vythilingam, M., Pessoa, L., Fridberg, D, Zametkin, A, Nelson, E.E., Drevets, W.C., Pine, D.S, Martin, A & Blair, R.J.R. (2007). Modulation of emotion by cognition and cognition by emotion. *NeuroImage*, *35*(1), 430–440. doi:10.1016/j.neuroimage.2006.11.048

Brett, M., Penny, W., & Kiebel, S. (2004). An Introduction to Random Field Theory. In R. S. J. Frackowiak, K. Friston, & C. Frith (Eds.), *Human Brain Function* (2nd ed., pp. 867–880). Amsterdam; Boston: Elsevier Academic Press.

Brett, M., Anton, J.-L., Valabregue, R., & Poline, J.-B. (2002). Region of interest analysis using an SPM toolbox: (abstract). *8th International Conference on Functional Brain Mapping of the Human Brain*. Available on CD-ROM in *NeuroImage*, 16(2).

Brühl, A. B., Rufer, M., Delsignore, A., Kaffenberger, T., Jäncke, L., & Herwig, U. (2011). Neural correlates of altered general emotion processing in social anxiety disorder. *Brain Research*, *1378*, 72–83. doi:10.1016/j.brainres.2010.12.084

Buxton, R. B., Wong, E. C., & Frank, L. R. (1998). Dynamics of blood flow and oxygenation changes during brain activation: the Balloon model. *Magnetic resonance in medicine: official journal of the Society of Magnetic Resonance in Medicine / Society of Magnetic Resonance in Medicine*, *39*(6), 855–864.

Cannon, W. (1927). The James-Lange Theory of Emotions: A Critical Examination and an Alternative Theory. *The American Journal of Psychology*, *39*, 106–124.

Chawla, D., Rees, G., & Friston, K. J. (1999). The physiological basis of attentional modulation in extrastriate visual areas. *Nature Neuroscience*, *2*(7), 671–676. doi:10.1038/10230

Clark, D. M., & Wells, A. (1995). A cognitive model of social phobia. In R. G. Heimberg, F. R. Schneier, & M. R. Liebowitz (Eds.), *Social phobia. Diagnosis, assessment, and treatment* (pp. 69–93). New York: Guilford Press.

Cooney, R. E., Atlas, L. Y., Joormann, J., Eugène, F., & Gotlib, I. H. (2006). Amygdala activation in the processing of neutral faces in social anxiety disorder: Is neutral really neutral? *Psychiatry Research: Neuroimaging*, *148*(1), 55–59. doi:10.1016/j.pscychresns.2006.05.003

Damasio, A. R. (1994). *Descartes' error: Emotion, reason, and the human brain*. New York: Avon Books.

Daunizeau, J., David, O., & Stephan, K. E. (2011). Dynamic causal modelling: a critical review of the biophysical and statistical foundations. *NeuroImage*, *58*(2), 312–322. doi:10.1016/j.neuroimage.2009.11.062

Davis, M., & Whalen, P. J. (2001). The amygdala: vigilance and emotion. *Molecular psychiatry*, *6*(1), 13–34.

Deichmann, R. (2009). Principles of MRI and Functional MRI. In M. Filippi (Ed.), *FMRI techniques and protocols* (pp. 3–30). New York [etc.]: Springer.

Ding, J., Chen, H., Qiu, C., Liao, W., Warwick, J. M., Duan, X., Zhang, W. & Gong, Q. (2011). Disrupted functional connectivity in social anxiety disorder: a resting-state fMRI study. *Magnetic Resonance Imaging*, *29*(5), 701–711. doi:10.1016/j.mri.2011.02.013

Fehm, L., Pelissolo, A., Furmark, T., & Wittchen, H.-U. (2005). Size and burden of social phobia in Europe. *European Neuropsychopharmacology*, *15*(4), 453–462. doi:10.1016/j.euroneuro.2005.04.002

Fenker, D. B., Heipertz, D., Boehler, C. N., Schoenfeld, M. A., Noesselt, T., Heinze, H.-J., Duezel, E. & Hopf, J.M. (2010). Mandatory processing of irrelevant fearful face features in visual search. *Journal of cognitive neuroscience*, *22*(12), 2926–2938. doi:10.1162/jocn.2009.21340

FIL Methods Group. (2012). *SPM8 Manual*. Retrieved from http://www.fil.ion.ucl.ac.uk/spm/

First, M. B., Spitzer, R. L., Gibbon, M., & Williams, J. B. (1996). *Structured Clinical Interview for DSM-IV*. Washington, DC: American Psychiatric Association.

Friston, K. J. (2009). Dynamic Causal Modelling of Brain Responses. In M. Filippi (Ed.), *FMRI techniques and protocols* (pp. 237–261). New York [etc.]: Springer.

Friston, K. J. (2011). Functional and Effective Connectivity: A Review. *Brain Connectivity*, *1*(1), 13–36. doi:10.1089/brain.2011.0008

Friston, K. J., Harrison, L., & Penny, W. (2003). Dynamic causal modelling. *NeuroImage*, *19*(4), 1273–1302.

Friston, K. J., Josephs, O., Rees, G., & Turner, R. (1998). Nonlinear event-related responses in fMRI. *Magnetic Resonance in Medicine*, *39*(1), 41–52. doi:10.1002/mrm.1910390109

Garavan, H., & Murphy, K. (2009). Experimental design. In M. Filippi (Ed.), *FMRI techniques and protocols* (pp. 133–149). New York [etc.]: Springer.

Glascher, J., & Adolphs, R. (2003). Processing of the arousal of subliminal and supraliminal emotional stimuly by the human amygdala. *Journal of Neuroscience*, *23*, 439–447.

Glaser, D., Friston, K., Mechelli, A., Turner, R., & Price, C. (2004). Hemodynamic Modelling. In R. S. J. Frackowiak, K. Friston, & C. Frith (Eds.), *Human Brain Function* (2nd ed., pp. 823–842). Amsterdam; Boston: Elsevier Academic Press.

Hahn, A., Stein, P., Windischberger, C., Weissenbacher, A., Spindelegger, C., Moser, E., Kasper, S. & Lanzengerger, R. (2011). Reduced resting-state functional connectivity between amygdala and orbitofrontal cortex in social anxiety disorder. *NeuroImage*, *56*(3), 881–889. doi:10.1016/j.neuroimage.2011.02.064

Hamilton, M. (1959). The assessment of anxiety states by rating. *The British journal of medical psychology*, *32*(1), 50–55.

Henson, R. (2004). Analysis of fMRI time-series: Linear Time-Invariant models, event-related fMRI and optimal experimental design. In R. S. J. Frackowiak, K. Friston, & C. Frith (Eds.), *Human Brain Function* (2nd ed., pp. 793–822). Amsterdam; Boston: Elsevier Academic Press.

Henson, R. (2007). Efficient experimental design for fMRI. In K. J. Friston, J. Ashburner, S. Kiebel, & W. Penny (Eds.), *Statistical parametric mapping. The analysis of functional brain images* (pp. 193–210). London: Academic.

Hoffman, E. J., & Mathew, S. J. (2008). Anxiety disorders: a comprehensive review of pharmacotherapies. *The Mount Sinai journal of medicine, New York*, *75*(3), 248–262. doi:10.1002/msj.20041

Hofmann, S. G., & Smits, J. A. J. (2008). Cognitive-behavioural therapy for adult anxiety disorders: a meta-analysis of randomized placebo-controlled trials. *The Journal of clinical psychiatry*, *69*(4), 621–632.

IBM Corp. Released 2011. IBM SPSS Statistics for Windows. Version 20.0. Armonk, NY: IBM Corp.

Kashdan, T. B., & McKnight, P. E. (2010). The Darker Side of Social Anxiety: When Aggressive Impulsivity Prevails Over Shy Inhibition. *Current Directions in Psychological Science*, *19*(1), 47–50. doi:10.1177/0963721409359280

Kendler, K. S., Karkowski, L. M., & Prescott, C. A. (1999). Fears and phobias: reliability and heritability. *Psychological medicine*, *29*(3), 539–553.

Klumpp, H., Angstadt, M., & Phan, K. L. (2012). Insula reactivity and connectivity to anterior cingulate cortex when processing threat in generalized social anxiety disorder. *Biological Psychology*, *89*(1), 273–276. doi:10.1016/j.biopsycho.2011.10.010

Krain, A. L., Gotimer, K., Hefton, S., Ernst, M., Castellanos, F. X., Pine, D. S., & Milham, M. P. (2008). A Functional Magnetic Resonance Imaging Investigation of Uncertainty in Adolescents with Anxiety Disorders. *Biological Psychiatry*, *63*(6), 563–568. doi:10.1016/j.biopsych.2007.06.011

Labuschagne, I., Phan, K. L., Wood, A., Angstadt, M., Chua, P., Heinrichs, M., Stout, J.C. & Nathan, P.J. (2011). Medial frontal hyperactivity to sad faces in generalized social anxiety disorder and modulation by oxytocin. *International Journal of Neuropsychopharmacology*, (14), 1–14.

Lanzenberger, R. R., Mitterhauser, M., Spindelegger, C., Wadsak, W., Klein, N., Mien, L.-K., Holik, A., Attarbaschi, T., Mossaheb, N., Sacher, J., Geiss-Granadia, T., Kletter, K., Kasper, S. & Tauscher, J. (2007). Reduced serotonin-1A receptor binding in social anxiety disorder. *Biological psychiatry*, *61*(9), 1081–1089. doi:10.1016/j.biopsych.2006.05.022

Lautenbur, P. C. (1973). Image Formation by Induced Local Interactions: Examples Employing Nuclear Magnetic Resonance. *Nature*, *242*(5394), 190–191. doi:10.1038/242190a0

Lazar, N. A. (2008). *The statistical analysis of functional MRI data*. New York: Springer.

Lazarus, R. S. (1981). A cognitivist's reply to Zajonc on emotion and cognition. *American Psychologist*, *36*(2), 222–223. doi:10.1037/0003-066X.36.2.222

LeDoux, J. E. (1984). Cognition and emotion: Processing functions and brain systems. In M. S. Gazzaniga (Ed.), *Handbook of cognitive neuroscience* (pp. 267–289). New York: Plenum Press.

LeDoux, J. E. (2000). Emotion Circuits in the Brain. *Annual Review of Neuroscience*, *23*(1), 155–184. doi:10.1146/annurev.neuro.23.1.155

Liang, Z.-P., & Lauterbur, P. C. (2000). *Principles of magnetic resonance imaging: A signal processing perspective*. Bellingham, Wash, New York: SPIE Optical Engineering Press; IEEE Press.

Liao, W., Chen, H., Feng, Y., Mantini, D., Gentili, C., Pan, Z., Ding, J., Duan, X., Qiu, C., Lui, S., Gong, Q. & Zhang, W. (2010). Selective aberrant functional connectivity of resting state networks in social anxiety disorder. *NeuroImage*, *52*(4), 1549–1558. doi:10.1016/j.neuroimage.2010.05.010

Li, D., Chokka, P., & Tibbo, P. (2001). Toward an integrative understanding of social phobia. *Journal of psychiatry & neuroscience : JPN*, *26*(3), 190–202.

Liebowitz, M. R. (1987). Social phobia. *Modern problems of pharmacopsychiatry*, *22*, 141–173.

Lindquist, M. A. (2008). The Statistical Analysis of fMRI Data. *Statistical Science*, *23*(4), 439–464. doi:10.1214/09-STS282

Ljunggren, S. (1983). A simple graphical representation of Fourier-based imaging methods. *Journal of Magnetic Resonance*, (53), 338–343.

Logothetis, N. K. (2002). The neural basis of the blood-oxygen-level-dependent functional magnetic resonance imaging signal. *Philosophical Transactions of the Royal Society B: Biological Sciences*, *357*(1424), 1003–1037. doi:10.1098/rstb.2002.1114

Lohmann, G., Erfurth, K., Müller, K., & Turner, R. (2012). Critical comments on dynamic causal modelling. *NeuroImage*, *59*(3), 2322–2329. doi:10.1016/j.neuroimage.2011.09.025

Mancini, C., van Ameringen, M., Szatmari, P., Fugere, C., & Boyle, M. (1996). A high-risk pilot study of the children of adults with social phobia. *Journal of the American Academy of Child and Adolescent Psychiatry*, *35*(11), 1511–1517. doi:10.1097/00004583-199611000-00020

Mantella, R. C., Butters, M. A., Amico, J. A., Mazumdar, S., Rollman, B. L., Begley, A. E., Reynolds, C.F & Lenze, E. J. (2008). Salivary cortisol is associated with diagnosis and severity of late-life generalized anxiety disorder. *Psychoneuroendocrinology*, *33*(6), 773–781. doi:10.1016/j.psyneuen.2008.03.002

Markowitsch, H. J. (1998). Differential contribution of right and left amygdala to affective information processing. *Behavioural Neurology*, *11*(233-244).

Martel, F. L., Hayward, C., Lyons, D. M., Sanborn, K., Varady, S., & Schatzberg, A. F. (1999). Salivary cortisol levels in socially phobic adolescent girls. *Depression and anxiety*, *10*(1), 25–27.

Mellings, T. M., & Alden, L. E. (2000). Cognitive processes in social anxiety: the effects of self-focus, rumination and anticipatory processing. *Behaviour research and therapy*, *38*(3), 243–257.

Mitchell, D. G. V., Nakic, M., Fridberg, D., Kamel, N., Pine, D. S., & Blair, R. J. R. (2007). The impact of processing load on emotion. *NeuroImage*, *34*(3), 1299–1309. doi:10.1016/j.neuroimage.2006.10.012

Monk, C. S., Telzer, E. H., Mogg, K., Bradley, B. P., Mai, X., Louro, H. M., Chen, G., McClure-Tone, E. B., Ernst, M. & Pine, D. S. (2008). Amygdala and ventrolateral prefrontal cortex activation to masked angry faces in children and adolescents with generalized anxiety disorder. *Archives of General Psychiatry*, *65*(5), 568–576.

Nakao, T., Sanematsu, H., Yoshiura, T., Togao, O., Murayama, K., Tomita, M., Masuda, Y., & Kanba, S. (2011). fMRI of patients with social anxiety disorder during a social situation task. *Neuroscience Research*, *69*(1), 67–72. doi:10.1016/j.neures.2010.09.008

Ochsner, K., & Gross, J. (2005). The cognitive control of emotion. *Trends in Cognitive Sciences*, *9*(5), 242–249. doi:10.1016/j.tics.2005.03.010

Ogawa, S., & Sung, Y.-W. (2007). Functional magnetic resonance imaging. *Scholarpedia*, *2*(10), 3105. doi:10.4249/scholarpedia.3105

Olmos, J. S. de, & Heimer, L. (1999). The concepts of the ventral striatopallidal system and extended amygdala. *Annals of the New York Academy of Sciences*, *877*, 1–32.

Pessoa, L., Padmala, S., & Morland, T. (2005). Fate of unattended fearful faces in the amygdala is determined by both attentional resources and cognitive modulation. *NeuroImage*, *28*(1), 249–255. doi:10.1016/j.neuroimage.2005.05.048

Petersen, S. E., & Dubis, J. W. (2012). The mixed block/event-related design. *NeuroImage*, *62*(2), 1177–1184. doi:10.1016/j.neuroimage.2011.09.084

Phan, K. L., Fitzgerald, D. A., Nathan, P. J., & Tancer, M. E. (2006). Association between Amygdala Hyperactivity to Harsh Faces and Severity of Social Anxiety in Generalized Social Phobia. *Biological Psychiatry*, *59*(5), 424–429. doi:10.1016/j.biopsych.2005.08.012

Phelps, E. A., & LeDoux, J. E. (2005). Contributions of the amygdala to emotion processing: from animal models to human behavior. *Neuron*, *48*(2), 175–187. doi:10.1016/j.neuron.2005.09.025

Phelps, E. A., O'Connor, K. J., Gatenby, J. C., Gore, J. C., Grillon, C., & Davis, M. (2001). Activation of the left amygdala to a cognitive representation of fear. *Nature Neuroscience*, *4*, 437–441.

Phillips, M. L., Ladouceur, C. D., & Drevets, W. C. (2008). A neural model of voluntary and automatic emotion regulation: implications for understanding the pathophysiology and neurodevelopment of bipolar disorder. *Molecular psychiatry*, *13*(9), 829, 833-57. doi:10.1038/mp.2008.65

Plutchik, R. (2003). *Emotions and life: Perspectives from psychology, biology, and evolution* (1st ed.). Washington, DC: American Psychological Association.

Poldrack, R. A., Mumford, J. A., & Nichols, T. E. (2011). *Handbook of functional MRI data analysis*. New York: Cambridge University Press.

Posner, M. I., & Petersen, S. E. (1990). The attention system of the human brain. *Annual Review of Neuroscience*, *13*, 25–42. doi:10.1146/annurev.ne.13.030190.000325

Power, M. J., & Dalgleish, T. (2008). *Cognition and emotion: From order to disorder* (2nd ed.). Hove [England] ;, New York: Psychology Press.

Qiu, C., Liao, W., Ding, J., Feng, Y., Zhu, C., Nie, X., Zhang, W., Chen, H., & Gong, O. (2011). Regional homogeneity changes in social anxiety disorder: A resting-state fMRI study. *Psychiatry Research: Neuroimaging*, *194*(1), 47–53. doi:10.1016/j.pscychresns.2011.01.010

Rabi, I., Zacharias, J., Millman, S., & Kusch, P. (1938). A New Method of Measuring Nuclear Magnetic Moment. *Physical Review*, *53*(4), 318. doi:10.1103/PhysRev.53.318

Rapee, R. M., & Heimberg, R. G. (1997). A cognitive-behavioral model of anxiety in social phobia. *Behaviour research and therapy*, *35*(8), 741–756.

Robinson, S., Windischberger, C., Rauscher, A., & Moser, E. (2004). Optimized 3 T EPI of the amygdalae. *NeuroImage*, *22*(1), 203–210. doi:10.1016/j.neuroimage.2003.12.048

Ruscio, A. M., Brown, T. A., Chiu, W. T., Sareen, J., Stein, M. B., & Kessler, R. C. (2008). Social fears and social phobia in the USA: results from the National Comorbidity Survey Replication. *Psychological medicine*, *38*(1), 15–28. doi:10.1017/S0033291707001699

Schachter, S., & Singer, J. E. (1962). Cognitive, social, and physiological determinants of emotional state. *Psychological review*, *69*, 379–399.

Schneier, F. R., Kent, J. M., Star, A., & Hirsch, J. (2009). Neural circuitry of submissive behavior in social anxiety disorder: A preliminary study of response to direct eye gaze. *Psychiatry Research: Neuroimaging*, *173*(3), 248–250. doi:10.1016/j.pscychresns.2008.06.004

Schneier, F. R., Liebowitz, M. R., Abi-Dargham, A., Zea-Ponce, Y., Lin, S. H., & Laruelle, M. (2000). Low dopamine D(2) receptor binding potential in social phobia. *The American journal of psychiatry*, *157*(3), 457–459.

Schneier, F. R., Pomplun, M., Sy, M., & Hirsch, J. (2011). Neural response to eye contact and paroxetine treatment in generalized social anxiety disorder. *Psychiatry Research: Neuroimaging*, *194*(3), 271–278. doi:10.1016/j.pscychresns.2011.08.006

Schultz, L. T., & Heimberg, R. G. (2008). Attentional focus in social anxiety disorder: Potential for interactive processes. *Clinical Psychology Review*, *28*(7), 1206–1221. doi:10.1016/j.cpr.2008.04.003

Schupp, H. T., Junghöfer, M., Weike, A. I., & Hamm, A. O. (2003). Attention and emotion: an ERP analysis of facilitated emotional stimulus processing. *Neuroreport*, *14*(8), 1107–1110. doi:10.1097/01.wnr.0000075416.59944.49

Shields, S. A., & Kappas, A. (2006). *Magda B. Arnold's contributions to emotion research and theory*. Hove: Psychology Press.

Silvert, L., Lepsien, J., Fragopanagos, N., Goolsby, B., Kiss, M., Taylor, J. G., Raymond, J. E., Shapiro, K. L., Eimer, M., & Nobre, A. C. (2007). Influence of attentional demands on the processing of emotional facial expressions in the amygdala. *NeuroImage*, *38*(2), 357–366. doi:10.1016/j.neuroimage.2007.07.023

Sladky, R., Höflich, A., Atanelov, J., Kraus, C., Baldinger, P., Moser, E., Lanzenberger, R., & Windischberger, C. (2012). Increased neural habituation in the amygdala and orbitofrontal cortex in social anxiety disorder revealed by fMRI. *PLoS ONE*, *7*(11), 1–9.

Sladky, R., Friston, K. J., Tröstl, J., Cunnington, R., Moser, E., & Windischberger, C. (2011). Slice-timing effects and their correction in functional MRI. *NeuroImage*, *58*(2), 588–594. doi:10.1016/j.neuroimage.2011.06.078

Spielberger, C., Gorssuch, R., Lushene, P., Vagg, P., & Jacobs, G. (1983). *Manual for the State-Trait Anxiety Inventory*. Palo Alto: Consulting Psychologists Press, Inc.

Stein, J. L., Wiedholz, L. M., Bassett, D. S., Weinberger, D. R., Zink, C. F., Mattay, V. S., & Meyer-Lindenberg, A. (2007). A validated network of effective amygdala connectivity. *NeuroImage*, *36*(3), 736–745. doi:10.1016/j.neuroimage.2007.03.022

Stein, M. B. (2002). Increased Amygdala Activation to Angry and Contemptuous Faces in Generalized Social Phobia. *Archives of General Psychiatry*, *59*(11), 1027–1034. doi:10.1001/archpsyc.59.11.1027

Stein, M. B., Chartier, M. J., Hazen, A. L., Kozak, M. V., Tancer, M. E., Lander, S., Furer, P., Chubaty, D., & Walker, J. R. (1998). A direct-interview family study of generalized social phobia. *The American journal of psychiatry*, *155*(1), 90–97.

Stephan, K. E., Harrison, L. M., Kiebel, S. J., David, O., Penny, W. D., & Friston, K. J. (2007). Dynamic causal models of neural system dynamics:current state and future extensions. *Journal of biosciences*, *32*(1), 129–144.

Stephan, K. E., Penny, W., Moran, R., den Ouden, H., Daunizeau, J., & Friston, K. (2010). Ten simple rules for dynamic causal modeling. *NeuroImage*, *49*(4), 3099–3109. doi:10.1016/j.neuroimage.2009.11.015

Tiihonen, J., Kuikka, J., Bergström, K., Lepola, U., Koponen, H., & Leinonen, E. (1997). Dopamine reuptake site densities in patients with social phobia. *The American journal of psychiatry*, *154*(2), 239–242.

Tillfors, M., Furmark, T., Marteinsdottir, I., Fischer, H., Pissiota, A., Langstroem, B., & Fredrikson, M. (2001). Cerebral blood flow in subjects with social phobia during stressful speaking tasks: a PET study. *The American journal of psychiatry*, *158*(8), 1220–1226.

Tröstl, J., Sladky, R., Hummer, A., Kraus, C., Moser, E., Kasper, S., Lanzenberger, R., & Windischberger, C. (2011). P01-182 - Reduced connectivity in the uncinate fiber tract between the frontal cortex and limbic subcortical areas in social phobia. *European Psychiatry*, *26*, 182. doi:10.1016/S0924-9338(11)71893-4

Twieg, D. B. (1983). The k-trajectory formulation of the NMR imaging process with applications in analysis and synthesis of imaging methods. *Medical Physics*, *10*(5), 610. doi:10.1118/1.595331

Uhde, T. W., Tancer, M. E., Gelernter, C. S., & Vittone, B. J. (1994). Normal urinary free cortisol and postdexamethasone cortisol in social phobia: comparison to normal volunteers. *Journal of affective disorders*, *30*(3), 155–161.

van der Wee, N. J., van Veen, J. F., Stevens, H., van Vliet, I. M., van Rijk, P. P., & Westenberg, H. G. (2008). Increased Serotonin and Dopamine Transporter Binding in Psychotropic Medication-Naive Patients with Generalized Social Anxiety Disorder Shown by 123I- -(4-Iodophenyl)-Tropane SPECT. *Journal of Nuclear Medicine*, *49*(5), 757–763. doi:10.2967/jnumed.107.045518

Vaswani, M., Linda, F. K., & Ramesh, S. (2003). Role of selective serotonin reuptake inhibitors in psychiatric disorders: a comprehensive review. *Progress in neuro-psychopharmacology & biological psychiatry*, *27*(1), 85–102.

Vul, E., Harris, C., Winkielman, P., & Pashler, H. (2009). Puzzlingly High Correlations in fMRI Studies of Emotion, Personality, and Social Cognition. *Perspectives on Psychological Science*, *4*(3), 274–290. doi:10.1111/j.1745-6924.2009.01125.x

Warwick, J. M., Carey, P. D., Cassimjee, N., Lochner, C., Hemmings, S., Moolman-Smook, H., Beetge, E., Dupont, P, & Stein, D. J. (2012). Dopamine transporter binding in social anxiety disorder: the effect of treatment with escitalopram. *Metabolic brain disease*, *27*(2), 151–158. doi:10.1007/s11011-012-9280-3

Whalen, P. J., Rauch, S. L., Etcoff, N. L., McInerney, S. C., Lee, M. B., & Jenike, M. A. (1998). Masked presentations of emotional facial expressions modulate amygdala activity without explicit knowledge. *The Journal of Neuroscience: the official journal of the Society for Neuroscience*, *18*(1), 411–418.

Williams, J. M. G. (1997). *Cognitive psychology and emotional disorders* (2nd ed.). Chichester ;, New York: Wiley.

Willner, P., Hale, A. S., & Argyropoulos, S. (2005). Dopaminergic mechanism of antidepressant action in depressed patients. *Journal of affective disorders*, *86*(1), 37–45. doi:10.1016/j.jad.2004.12.010

Wittchen, H., Jacobi, F., Rehm, J., Gustavsson, A., Svensson, M., Jönsson, B.,Olesen, J, Allgulander, C., Alonso, J., Faravelli, C., Fratiglioni, L., Jennum, P., Lieb, R., Maercker, A., van Os, J., Preisig, M., Salvador-Carulla, L., Simon, R., & Steinhausen, H. C. (2011). The size and burden of mental disorders and other disorders of the brain in Europe 2010. *European Neuropsychopharmacology*, *21*(9), 655–679. doi:10.1016/j.euroneuro.2011.07.018

Wittchen, H.-U., & Fehm, L. (2003). Epidemiology and natural course of social fears and social phobia. *Acta Psychiatrica Scandinavica*, *108*(s417), 4–18. doi:10.1034/j.1600-0447.108.s417.1.x

Woolrich, M. W., Beckmann, C. F., Nichols, T. E., & Smith, S. M. (2009). Statistical Analysis of fMRI Data. In M. Filippi (Ed.), *FMRI techniques and protocols* (pp. 179–236). New York [etc.]: Springer.

Worsley, K. J., Marrett, S., Neelin, P., Vandal, A. C., Friston, K. J., & Evans, A. C. (1996). A unified statistical approach for determining significant signals in images of cerebral activation. *Human brain mapping*, *4*(1), 58–73. doi:10.1002/(SICI)1097-0193(1996)4:1<58::AID-HBM4>3.0.CO;2-O

Wright, C. I., Fischer, H., Whalen, P. J., McInerney, S., Shin, L. M., & Rauch, S. L. (2001). Differential prefrontal cortex and amygdala habituation to repeatedly presented emotional stimuli. *Neuroreport*, *12*, 379–383.

Zajonc, R. B. (1980). Feeling and thinking: Preferences need no inferences. *American Psychologist*, *35*(2), 151–175. doi:10.1037/0003-066X.35.2.151

# Curriculum Vitae

**Personal Information**

| | |
|---|---|
| Name | Lora Guintcheva Minkova |
| Date of birth | 16.09.1984 |
| Place of birth | Sofia, Bulgaria |

**Education**

| | |
|---|---|
| since 11/2012 | PhD student in Psychology, University of Freiburg |
| since 10/2010 | M.Sc. student in Cognitive Science, University of Vienna |
| 10/2004 – 08/2010 | M.A. in English Studies, Dresden University of Technology |

**Employment**

| | |
|---|---|
| since 11/2012 | PhD Research Assistant<br>Freiburg Brain Imaging, University Medical Center Freiburg |

**Other Research Projects**

| | |
|---|---|
| since 11/2012 | Dissertation: *Investigating the Early Changes in the Neuroanatomy and Cognitive Function Associated with Huntington's Disease*<br>Supervisors: Prof. Dr. Markus Heinrichs, University of Freiburg & PD Dr. Stefan Klöppel, MD, University Medical Center Freiburg |
| 09/2011 – 03/2012 | Project: *ERP Measure of Automatic Number Processing*<br>Supervisor: Dr. Marijan Palmovic, University of Zagreb |
| 02/2011 – 08/2011 | Project: *Distribution of GABA-A Receptor Subunits in Epileptic Patients*<br>Supervisors: Harald Stefanits, MD & Ivan Milenkovic, MD, Medical University of Vienna |
| 02/2010 – 08/2010 | Master thesis: *Anglicisms in the Bulgarian Printed Press after 1989*<br>Supervisors: Prof. Dr. Ursula Schaefer & Prof. Dr. Holger Kuße, Dresden University of Technology |